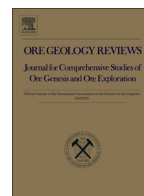




ELSEVIER

Contents lists available at ScienceDirect

Ore Geology Reviews

journal homepage: [www.elsevier.com/locate/oregeorev](http://www.elsevier.com/locate/oregeorev)

## Comparing prospectivity modelling results and past exploration data: A case study of porphyry Cu–Au mineral systems in the Macquarie Arc, Lachlan Fold Belt, New South Wales

Oliver P. Kreuzer<sup>a,b,c,\*</sup>, Alexandra V.M. Miller<sup>d</sup>, Katie J. Peters<sup>d</sup>, Constance Payne<sup>d</sup>, Charlene Wildman<sup>d</sup>, Gregor A. Partington<sup>d</sup>, Elisa Puccioni<sup>d</sup>, Maureen E. McMahon<sup>c</sup>, Michael A. Etheridge<sup>c</sup>

<sup>a</sup> X-plore Geoconsulting, 39 Morrill Close, Rockingham, WA 6168, Australia

<sup>b</sup> Economic Geology Research Centre (EGRU), School of Earth & Environmental Science, James Cook University, Townsville, QLD 4811, Australia

<sup>c</sup> ARC National Key Centre for Geochemical Evolution and Metallogeny of Continents (GEMOC), Department of Earth and Planetary Sciences, Macquarie University, North Ryde, NSW 2109, Australia

<sup>d</sup> Kenex Ltd, PO Box 41136, Eastbourne, Wellington, New Zealand

### ARTICLE INFO

#### Article history:

Received 24 May 2014

Received in revised form 23 August 2014

Accepted 1 September 2014

Available online xxxx

#### Keywords:

Mineral prospectivity modelling

Exploration targeting

Mineral systems approach

Efficiency of mineral exploration

Porphyry Cu–Au

Macquarie Arc

Lachlan Fold Belt

### ABSTRACT

Mineral exploration is undertaken in stages, with each stage designed to get to the next decision point of whether or not to keep exploring a particular area based on the results at hand. As a general rule, each consecutive exploration stage is more expensive due to the progressively more drill- and study-intensive nature of the work required, in particular after discovery of a potentially economic mineral deposit. As such, the distribution of exploration activities and related expenditures essentially serve as a spatial measure of prospectivity as perceived by mineral exploration companies. In this study we compare historic (1980 to 2002) porphyry Cu–Au exploration activities and expenditures in part of the Ordovician to Early Silurian Macquarie Arc, Australia's most significant porphyry province with total resources greater than 80 Moz of Au and 13 Mt of Cu, to prospectivity modelling results from a weights of evidence (WofE) model. The outcomes of this spatial and statistical comparison indicate that at 2002 the Macquarie Arc was by no means a mature exploration destination and that past exploration investment outside the main mining areas was not necessarily effective. Moreover, no spatial correlation was apparent between areas of higher exploration expenditure and greater geological potential. For example, of the 692 km<sup>2</sup> of highly prospective ground covered by the exploration licences examined in this study, only 89 km<sup>2</sup> (c. 13%) have been explored effectively in that they received some form of drilling. Interestingly, the remaining area (603 km<sup>2</sup> or c. 87%) had not yet been effectively tested. As such, our analysis confirmed that despite a greater 100 year exploration and mining history, much of the prospective ground within the study area remained untested. Taken as a whole, the results of our spatial and statistical comparison are important inputs for assessing the effectiveness of exploration investment and exploration maturity and, therefore, future exploration decision-making. The outcomes also have implications for strategic planning of future government legislation helping to manage and maximise the benefits from exploration investment.

© 2014 Elsevier B.V. All rights reserved.

### 1. Introduction

Mineral prospectivity modelling with GIS (Bonham-Carter, 1994; Carranza, 2009) is increasingly being used by geoscientists in government and academia who, over the past 25 years, have significantly improved the various computational modelling techniques (e.g., weights of evidence, fuzzy logic, artificial neural networks: Porwal and Kreuzer, 2010) and applied them (i) to a wide range of mineral deposit types worldwide (González-Álvarez et al., 2010; Herbert

et al., 2014; Lindsay et al., 2014; Porwal et al., 2010), (ii) to data-rich and data-poor areas (Fallon et al., 2010; Ford and Hart, 2013; Lusty et al., 2012), and (iii) at scales typically ranging from district to continent (Billa et al., 2004; Feltrin, 2008; Nykänen et al., 2008). More recently the scope and capabilities of mineral prospectivity modelling have been significantly extended to include, for example, three dimensional analysis (Apel, 2006; Feltrin et al., 2008; McCaughey et al., 2009; Mejía-Herrera et al., 2014), fractal analysis (Ford and Blenkinsop, 2008; Wang et al., 2012), and economic risk analysis (Partington, 2009; Partington, 2010).

Regardless of these improvements and successes, uptake of GIS-based prospectivity modelling by industry has been slow (Partington and Sale, 2004); perhaps because the technique is (i) perceived as a

\* Corresponding author at: X-plore Geoconsulting, 39 Morrill Close, Rockingham, WA 6168, Australia. Tel.: +61 477 717 242.

E-mail address: [oliver@xploregeoconsulting.com](mailto:oliver@xploregeoconsulting.com) (O.P. Kreuzer).

black box technology that requires expert knowledge to operate, (ii) essentially interpolative and constrained by known data whilst most important exploration success has come from extrapolating patterns into environments of poor data coverage (Porwal and Kreuzer, 2010), (iii) typically applied to two-dimensional datasets whereas mineralisation processes operate in three-dimensional space (Porwal and Kreuzer, 2010), and (iv) rarely presented by its advocates as a practical tool for decision-making and problem-solving in mineral exploration. Whilst methodological and technical aspects of GIS-based prospectivity modelling have been dealt with comprehensively and published widely, demonstration of its practical applications has been very limited apart from the showcasing of mineral potential maps. These maps are very useful and informative but should not be regarded as the be-all and end-all of the modelling but as a starting point for further investigations.

Here we present an example of how a GIS-based prospectivity model may be used as input for further analysis. In this study, we compare prospectivity modelling results to real-world exploration data that essentially serve as a spatial measure of prospectivity as perceived by the minerals exploration industry (cf. Cowley et al., 2009). The outcomes of this spatial and statistical comparison have implications for assessing the effectiveness of exploration investment and exploration maturity, which are important inputs for future exploration decision-making. The outcomes also have implications for strategic planning of future government legislation helping to manage and maximise the benefits from exploration investment.

The area selected for the case study covers part of the Ordovician to Early Silurian Macquarie Arc (Fig. 1), a now dismembered intra-oceanic island arc most widely exposed in the Lachlan Fold Belt of New South Wales (Crawford et al., 2007; Glen, 2005; Hough et al., 2007). The Macquarie Arc is Australia's most fertile and productive porphyry province with an endowment of greater than 80 Moz of Au and 13 Mt of Cu (Clancy Exploration Limited, 2009; Cooke et al., 2007). The study area, which is defined by the Narromine, Dubbo, Forbes, Bathurst, Cootamundra, and Goulburn 1:250,000 scale map sheets, was selected to match an area investigated by a previous, unpublished study of historic porphyry Cu–Au exploration activities and expenditure commitments undertaken at the ARC National Key Centre for Geochemical Evolution and Metallogeny of Continents (GEMOC), Macquarie University, Sydney. A weights of evidence (WofE) model of porphyry Cu–Au prospectivity was developed by Kenex Limited in the framework of a mineral systems approach (Hronsky and Groves, 2008; Kreuzer et al., 2008; McCuaig et al., 2010; Wyborn et al., 1994). The model, which covers the entire Lachlan Fold Belt in New South Wales, was clipped to the study area, allowing direct comparison of the prospectivity model and the historic exploration and expenditure data.

## 2. Geology of the Macquarie Arc

The Ordovician to Early Silurian Macquarie Arc (Fig. 1) is an intra-oceanic island arc that is most-widely exposed in the New South Wales section of the Lachlan Fold Belt, one of five Palaeozoic orogenic belts in eastern Australia that together form the Tasman Fold Belt System (Foster and Gray, 2000; Glen, 2005; Hough et al., 2007; Supple and Scheibner, 1990; Walshe et al., 1995).

The Macquarie Arc performed a key role in the development of the Lachlan Fold Belt, which formed by complex accretionary processes

from Cambrian to Carboniferous times. These processes were triggered and sustained by the closure of the Wagga back-arc basin and associated collision of the Macquarie Arc with the proto-Pacific margin of Gondwanaland during the Late Ordovician to Early Silurian Benambra Orogeny. Post accretion, the Macquarie Arc was dismembered largely by E–W extension, with arc-parallel strike-slip faulting mainly restricted to the southern end. The overall tectonic development of the Macquarie Arc is commonly linked to its position above and interaction with a west-dipping subduction zone underneath the Gondwana plate, although a more complicated setting with multiple switches and intermittent cessation of subduction is likely (Cooke et al., 2007; Fergusson, 2009; Glen et al., 2007a; Holliday et al., 2002).

Igneous and volcanoclastic rocks of the now-dismembered Macquarie Arc are exposed in four structural belts:

- The Junee–Narromine Volcanic Belt in the west;
- The central Molong Volcanic Belt;
- The Rockley–Gulgong Volcanic Belt in the east; and
- The Kiandra Volcanic Belt in the south.

These belts, which formed by fragmentation of the Macquarie Arc post accretion, are separated by younger Silurian to Devonian rifts but can be correlated based on stratigraphy and major and trace element chemistry (Glen et al., 2007b, 2011).

Geochronological, stratigraphic and geochemical evidence is compatible with episodic evolution of the Macquarie Arc over a period of approximately 50 million years. The arc-related magmatism can be divided into four principal, partly overlapping phases that range in age from Early Ordovician to Early Silurian (Cooke et al., 2007; Crawford et al., 2007; Fergusson, 2009; Glen et al., 2007b):

- Phase 1 (Early Ordovician; c. 490 to 475 Ma): Produced mainly high-K calc-alkaline and shoshonitic intrusions and lavas that are only represented by relatively restricted outcrop in the Junee–Narromine and Molong volcanic belts.
- Phase 2 (Middle Ordovician; c. 466 to 450 Ma): Produced widespread, mainly high-K calc-alkaline and shoshonitic intrusions and lavas across all four structural belts of the arc.
- Phase 3 (Late Ordovician; c. 450 to 445 Ma): Produced shoshonitic intrusions and widespread but voluminously small, mainly felsic intrusions with distinctive medium-K calc-alkaline compositions; coincided with a five million year hiatus in magmatism in the western part of the arc that was accompanied by uplift, erosion and establishment of a widespread carbonate platform; resulted in the emplacement of porphyries and related Cu–Au mineralisation at Copper Hill, Cargo and possibly at Marsden.
- Phase 4 (Late Ordovician to Early Silurian; c. 458 to 437 Ma): Produced dominantly shoshonitic intrusions and lavas; coincided with crustal thickening during the Benambran Orogeny; resulted in the emplacement of the economically most significant Cu–Au mineralised porphyries in the Macquarie Arc.

Arc-related magmatism ceased in the Early Silurian during the protracted Benambran Orogeny (Cooke et al., 2007).

The Macquarie Arc is well endowed with large porphyry, skarn and epithermal deposits (cf. Table 1 in Cooke et al., 2007) containing more than 80 Moz of Au and 13 Mt of Cu (Clancy Exploration Limited, 2009). A spatial, temporal and genetic relationship is evident between many of the porphyry, skarn and epithermal deposits and Late Ordovician to Early Silurian shoshonitic intrusive complexes in the Macquarie

**Fig. 1.** Overview map illustrating the study areas: (1) Open-file, porphyry Cu–Au related exploration and expenditure data were compiled for the Narromine (SI/55-3), Dubbo (SI/55-4), Forbes (SI/55-7), Bathurst (SI/55-8), Cootamundra (SI/55-11), and Goulburn (SI/55-12) 1:250,000 scale map sheet areas (termed here the “GEMOC study”); (2) prospectivity analysis was carried out over the entire New South Wales portion of the Lachlan Fold Belt (termed here the “prospectivity study”) and clipped to the study area labelled (1). The map also shows the distribution of Ordovician to Early Silurian volcanic and intrusive rocks in the eastern Lachlan Fold Belt, known porphyry Cu–Au and related skarn deposits and major faults. The highly endowed Cadia and Northparkes porphyry Cu–Au districts are highlighted. Key to abbreviations, figure: CF = Copperhanna Fault, CNF = Coolac–Narromine Fault, EF = Ensay Fault, GF = Gilmore Fault, IF = Indi Fault, KF = Kiewa Fault, PF = Parkes Fault, YalF = Yalmy Fault, YarF = Yarralaw Fault. Key to abbreviations, inset: ACT = Australian Capital Territory, C = Canberra, LFB = Lachlan Fold Belt, NSW = New South Wales, S = Sydney, VIC = Victoria.

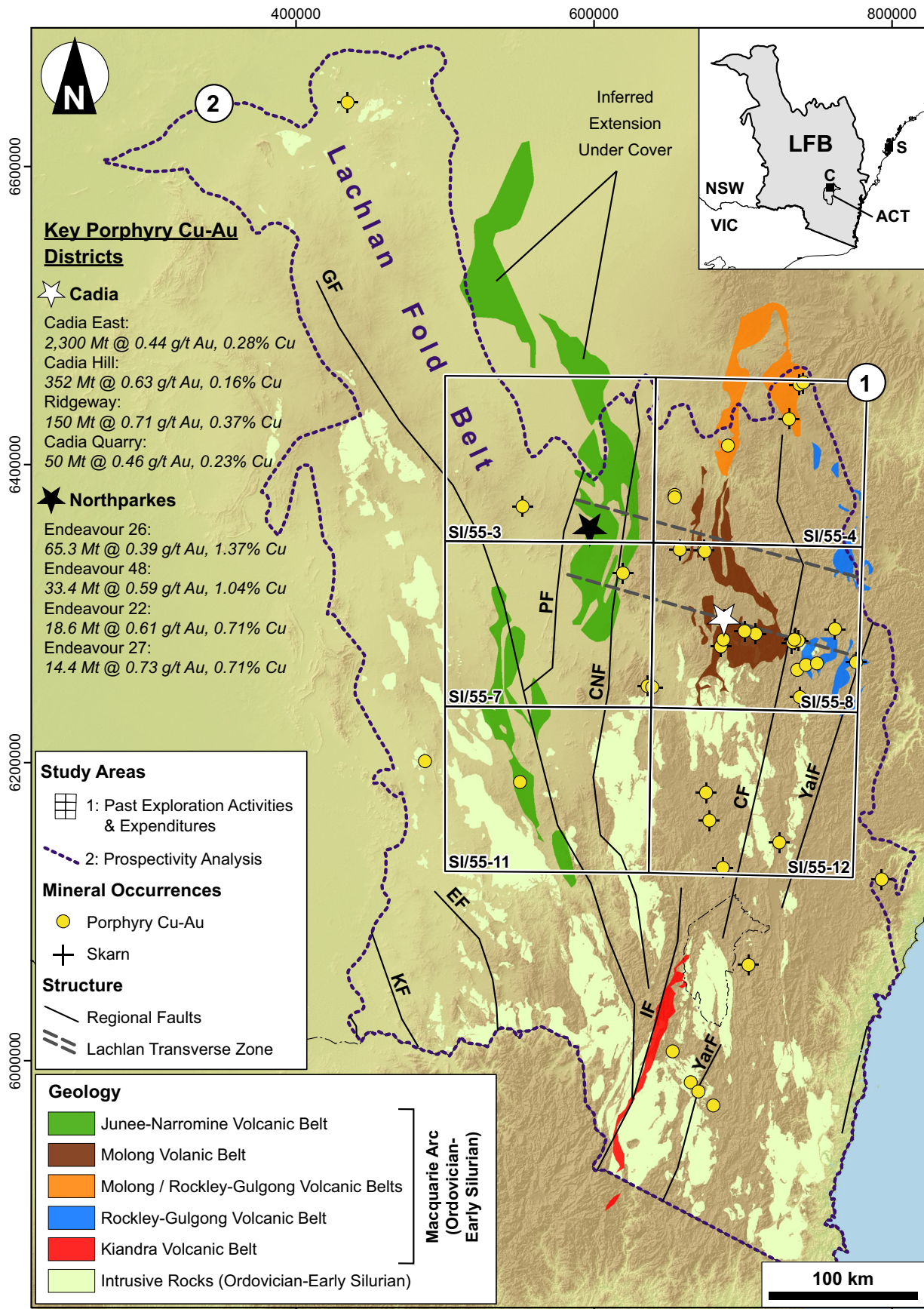


**Table 1**

Critical processes of the mineral system for porphyry Cu–Au and details of the WofE analysis of porphyry Cu–Au prospectivity for the Lachlan Fold Belt in New South Wales. See text for discussion.

Processes	Sub-processes	Mappable ingredients/ predictor maps	Classes	ID	Area (km <sup>2</sup> )	Units	N	W+	Ws+	W–	Ws–	C	Cs	Stud C	Comments
Source	(i) Melt generation in the mantle below the arc; (ii) mafic underplating; (iii) partial melting of lower crust; (iv) formation of crustal magma chambers; (v) extraction of metals from mantle and/or crustal sources	Proximity to Ordovician to Silurian felsic to intermediate intrusive and extrusive rocks	All rock types other than Ordovician to Silurian intrusive and extrusive rocks	1	147,329	73,664	4	–0.9	0.5	1.0	0.3	–1.9	0.6	–3.09	Lithological units were arranged into groups according to rock type (e.g., felsic intrusive rocks, intermediate intrusive rocks, felsic extrusive rocks, intermediate extrusive rocks) and age
			< 600 m from Ordovician to Silurian extrusive rocks (unless intrusive)	2	14,541	7270	2	0.7	0.7	–0.1	0.3	0.8	0.8	1.09	
			< 750 m from Ordovician to Silurian intrusive rocks	3	37,292	18,646	7	1.1	0.4	–0.6	0.4	1.6	0.6	2.92	
Transport	(i) Change in plate motion or angle of subduction, promoting extension, dilational deformation and vertical permeability; (ii) magma escape from crustal magma chamber; (iii) emplacement of porphyritic intrusions and/or dyke swarms to within 1 to 4 km of the surface	Proximity to areas of high fault density	Low density (within bottom 57/100 units)	1	187,542	93,771	6	–0.7	0.4	2.2	0.4	–2.9	0.6	–5.28	Fault density map (excluding thrust faults) was reclassified into 100 classes (100 = highest density, 0 = lowest density)
			Medium density (between 28 to 43/100 units)	2	7016	3508	2	1.5	0.7	–0.1	0.3	1.6	0.8	2.09	
			High density (within top 28/100 units)	3	4603	2301	5	2.8	0.4	–0.5	0.4	3.3	0.6	5.74	
Trap	(i) Stalling of magma ascent; (ii) exsolution of volatile phases from the cooling magma and consequential volume expansion and wallrock alteration; (iii) recurring fracturing and/or brecciation of enclosing country rocks driven by multiple intrusive events and magmatic-hydrothermal and/or tectonic processes	Proximity to magnetic highs	>1900 m from magnetic highs	1	154,005	77,003	3	–1.2	0.6	1.2	0.3	–2.5	0.7	–3.74	Domains of high total magnetic intensity (i.e., highs >56,432 nT) were extracted from the reclassified magnetic (TMI) data and buffered out to 5 km at 50 m intervals Calcareous lithological units of Silurian age or older were buffered out to 10 km at 100 m intervals Point theme of fault intersections (excluding thrust faults) was buffered by 2000 m around these points in 100 m intervals Point theme of fault bends (excluding thrust faults) was buffer by 4000 m at 100 m intervals around these points Lithological units were grouped according to competency contrast assigned on a range from 1 to 10; contacts between lithological units were extracted and further processes if the competency difference (d) was >3; contacts were buffered to 5 km at 100 m intervals Probability plots were created in ioGas to calculate Ag anomaly thresholds marked by breaks in rock chip assay value populations; the anomalous data were gridded using a 2000 m sphere of influence Probability plots were created in ioGas to calculate Au anomaly thresholds marked by breaks in rock chip assay value populations; the anomalous data were gridded using a 2000 m sphere of influence Probability plots were created in ioGas
			<1900 m from magnetic highs	2	45,156	22,578	10	1.2	0.3	–1.2	0.6	2.4	0.7	3.69	
		Proximity to calcareous rocks	>1400 m from calcareous rocks	1	195,054	97,527	10	–0.2	0.3	2.4	0.6	–2.7	0.7	–4.04	
			<1400 m from calcareous rocks	2	4108	2054	3	2.4	0.6	–0.2	0.3	2.7	0.7	4.04	
		Proximity to fault intersections	>2400 m from fault intersections	1	172,889	86,445	5	–0.8	0.4	1.5	0.4	–2.4	0.6	–4.13	
			<2400 m from fault intersections	2	26,272	13,136	8	1.5	0.4	–0.8	0.4	2.4	0.6	4.13	
		Proximity to fault bends	>1700 m from fault bends	1	184,300	92,150	7	–0.5	0.4	1.8	0.4	–2.4	0.6	–4.25	
			<1700 m from fault bends	2	14,861	7430	6	1.8	0.4	–0.5	0.4	2.4	0.6	4.25	
		Proximity to competency contrasts between lithological units	>1200 m from competency contrasts	1	181,309	90,655	8	–0.4	0.4	1.5	0.4	–1.8	0.6	–3.24	
			<1200 m from competency contrasts	2	17,852	8926	5	1.5	0.4	–0.4	0.4	1.8	0.6	3.24	
Deposition	(i) Transfer of metals into hydrothermal fluids that exsolved from the magma; (ii) fracture-controlled discharge of these metal-bearing hydrothermal fluids upwards and/or outwards from the magmatic source;	Proximity to Ag-in-rock chip anomalies	No data	–99	190,820	95,410	9	0.0	0.0	0.0	0.0	0.0	0.0	0.00	Probability plots were created in ioGas to calculate Ag anomaly thresholds marked by breaks in rock chip assay value populations; the anomalous data were gridded using a 2000 m sphere of influence Probability plots were created in ioGas to calculate Au anomaly thresholds marked by breaks in rock chip assay value populations; the anomalous data were gridded using a 2000 m sphere of influence Probability plots were created in ioGas
			<2000 m from Ag values <1 ppm	1	6095	3048	1	–1.1	1.0	1.0	0.6	–2.1	1.2	–1.82	
			<2000 m from Ag values >1 ppm	2	2246	1123	3	1.0	0.6	–1.1	1.0	2.1	1.2	1.82	
	Proximity to Au-in stream sediment anomalies	No data	–99	169,432	84,716	6	0.0	0.0	0.0	0.0	0.0	0.0	0.00		
		<1400 m from non-anomalous Au values	1	23,069	11,535	1	–1.7	1.0	1.3	0.4	–3.0	1.1	–2.81		
		<1400 m from anomalous Au values	2	6660	3330	6	1.3	0.4	–1.7	1.0	3.0	1.1	2.81		
(iv) outflow of spent fluids	Proximity to Cu-in-rock chip	No data	–99	164,327	82,164	5	0.0	0.0	0.0	0.0	0.0	0.00			

anomalies	<2000 m from Cu values <200 ppm	1	32,569	16,285	2	-1.3	0.7	2.5	0.4	-3.8	0.8	-4.61	to calculate Cu anomaly thresholds marked by breaks in rock chip assay value populations; the anomalous data were gridded using a 2000 m sphere of influence
	<2000 m from Cu values >200 ppm	2	2265	1132	6	2.5	0.4	-1.3	0.7	3.8	0.8	4.61	Gold occurrence data were used to compensate for the lack of gold assays in the drill hole and rock chip sample datasets
Proximity to Au occurrences	No data	-99	160,403	80,201	0	0.0	0.0	0.0	0.0	0.0	0.0	0.00	Domains of low total magnetic intensity (i.e., highs <56,104 nT; determined using natural breaks) were extracted from reclassified total magnetic intensity (TMI) data and buffered out to 5 km at 50 m intervals
	<2000 m from any mineral occurrence	1	14,632	7316	2	-0.9	0.7	0.3	0.3	-1.2	0.8	-1.57	Domains of strong magnetic gradient (difference >30 nT) were extracted from reclassified total magnetic intensity (TMI) raster data and buffered out to 5 km at 50 m intervals
	<2000 m from a Au occurrence	2	24,126	12,063	11	0.3	0.3	-0.9	0.7	1.2	0.8	1.57	
Proximity to magnetic lows	>350 m from magnetic lows	1	177,824	88,912	7	-0.5	0.4	1.5	0.4	-2.0	0.6	-3.53	
	<350 m from magnetic lows	2	21,337	10,669	6	1.5	0.4	-0.5	0.4	2.0	0.6	3.53	
Proximity to areas of strong magnetic gradient	>550 m from strong magnetic gradients	1	177,860	88,930	5	-0.8	0.4	1.8	0.4	-2.6	0.6	-4.55	
	<550 m from strong magnetic gradients	2	21,302	10,651	8	1.8	0.4	-0.8	0.4	2.6	0.6	4.55	

Arc (Holliday et al., 2002; Gray et al., 1995; Lickfold et al., 2003; Forster et al., 2004; Lawrie et al., 2007; Glen et al., 2007b; Cooke et al., 2007; Wilson et al., 2007; Forster, 2009).

### 3. Macquarie Arc porphyry Cu–Au deposits

#### 3.1. Alkalic porphyry Cu–Au deposits

The discovery of Cu and Au in the Macquarie Arc dates back to 1851. However, alkalic porphyry Cu–Au systems were only recognised in the Macquarie Arc in 1976 when wide-spaced drilling by Geopeko Limited intersected the Endeavour 22 deposit (Lye et al., 2006). Since then, two well-endowed clusters of Au-rich alkalic porphyries have been delineated in the Cadia (c. 40 Moz Au, 8 Mt Cu: Holliday et al., 2002; Thomas and Moorehead, 2011) and Northparkes (c. 2.1 Moz Au, 1.5 Mt Cu: Lickfold et al., 2003, 2007) districts. Combined, these districts constitute the world's second largest alkalic porphyry province after the Quesnel–Stikine terrane in British Columbia and the largest porphyry province in Australia (Cooke et al., 2007).

Mineralisation processes in the Cadia and Northparkes districts were centred upon composite, multiphase porphyritic monzonite intrusive complexes that intruded broadly comagmatic shoshonitic volcanic centres between 458 and 437 Ma at depths between 2 and 3 km. The locations of these districts are spatially coincident with a major NW–SE to WNW–ESE-striking basement structure cutting the Macquarie Arc obliquely. This structure, referred to as the Lachlan Transverse Zone, is thought to have favoured emplacement of porphyries by providing a favourable pathway for the migration of melts, leading to high-level ponding of magmas. The timing of this magmatism was synorogenic in that the porphyries intruded their tilted volcanic and volcanoclastic host sequences in the early phase of the Benambran Orogeny, after arc-related volcanism had effectively shut down and after the initial stages of accretion of the Macquarie Arc to Gondwana (Cooke et al., 2007; Glen et al., 2007b). Subsequent deformation partially dismembered the districts, thereby superposing different level porphyry Cu–Au systems and their host rocks (Thomas and Moorehead, 2011). Associated Late Ordovician to Middle Silurian uplift (at least 1 to 2 km) and erosion partially exhumed the porphyry Cu–Au systems (Cooke et al., 2007).

Cu–Au mineralisation in the Cadia district is spatially and genetically associated with alkalic, high K to shoshonitic intrusions of monzodiorite to quartz monzonite composition. The most significant deposits within the district are (Cooke et al., 2007; Smith, 2012):

- Cadia East (2300 Mt @ 0.44 g/t Au, 0.28% Cu);
- Cadia Hill (352 Mt @ 0.63 g/t Au, 0.16% Cu);
- Ridgeway (150 Mt @ 0.71 g/t Au, 0.37% Cu); and
- Cadia Quarry (50 Mt @ 0.46 g/t Au, 0.23% Cu).

Geochronological data suggest that the porphyry Cu–Au deposits in the Cadia district formed in two mineralising events separated by 18 million years and possibly younging eastwards, with Ridgeway being the oldest ( $456 \pm 6$  Ma) and Cadia East the youngest ( $438 \pm 3$  Ma) deposit in the district (Wilson et al., 2007). Mineralised intrusive bodies occur as small bosses, plugs and dykes that appear to emanate from a single batholith at depth, the presence of which is inferred from aeromagnetic data. Cu–Au mineralisation occurs as stockwork quartz veins, sheeted quartz veins and locally as broadly stratabound disseminations. Hydrothermal alteration associated with Cu–Au mineralisation is potassic, which is overprinted by selectively pervasive propylitic and silica–albite assemblages. To date, calc-alkalic porphyry Cu–Au mineralisation has been defined along a NW–SE-striking corridor six kilometres long and several hundred metres wide and has been traced by drilling to a depth of more than 1600 m (Holliday et al., 2002).

The Northparkes district comprises four economic porphyry Cu–Au deposits centred on narrow, pipelike quartz monzonite porphyry intrusive complexes, including

- Endeavour 26 (65.3 Mt @ 0.39 g/t Au, 1.37% Cu);
- Endeavour 48 (33.4 Mt @ 0.59 g/t Au, 1.04% Cu);
- Endeavour 22 (18.6 Mt @ 0.61 g/t Au, 0.71% Cu); and
- Endeavour 27 (14.4 Mt @ 0.73 g/t Au, 0.71% Cu).

Whilst these mineralised intrusions have vertical extents of at least 1400 m, they are among the smallest economic porphyry Cu–Au deposits in the world in terms of both tonnage and cross-sectional area (c. 300 by 200 m<sup>2</sup>) (Cooke et al., 2007; Lickfold et al., 2003). According to Lickfold et al. (2003), the Northparkes porphyry Cu–Au deposits, which formed between 446 Ma and 437 Ma, are remarkably consistent in terms of the sequences of intrusive emplacement, veining, and alteration. As such, it is possible that at the time of formation all four deposits were connected to a single mid- or upper-crustal magma chamber. Cu–Au mineralisation at the Northparkes deposits occurs as concentrically zoned, cylindrical bodies of quartz and sulphide stockwork veins centred on the multiphase quartz monzonite porphyry intrusive complexes. Hydrothermal alteration at Northparkes is typically restricted to within approximately 750 m of the intrusive host complexes and does not conform to the classic porphyry-style alteration zonation described by Lowell and Guilbert (1970). Rather, alteration assemblages are often discontinuous, non-symmetrical and do not all occur in every deposit.

### 3.2. Calc-alkalic porphyry Cu–Au deposits

In comparison with the alkalic porphyry Cu–Au systems in the Macquarie Arc, the calc-alkalic systems are poorly described (Champion et al., 2009). The most significant calc-alkalic porphyry deposits are Marsden (230 Mt @ 0.17 g/t Au, 0.34% Cu: Newcrest Mining Limited, 2014) and Copper Hill (153 Mt @ 0.28 g/t Au, 0.32% Cu: Golden Cross Resources Limited, 2013). Both are associated with calc-alkalic intrusive complexes of intrusive phase 3 that were emplaced between approximately 450 and 445 Ma. As such, they predate formation of the much larger alkalic porphyry systems of the Cadia and Northparkes districts by several millions of years (Cooke et al., 2007).

## 4. Mineral systems approach to porphyry Cu–Au mineralisation in the Macquarie Arc

### 4.1. The mineral systems approach

This study adopted a mineral systems approach to help constrain the work flow of this prospectivity analysis. The mineral systems approach is based on the premise that mineral deposits are the focal points of much larger earth process systems that operate on a variety of scales to focus mass and energy flux. Being process-based, the application of the mineral systems approach is neither restricted to a particular geological setting nor limited to a specific mineral deposit type. Rather, the flexibility of this concept allows for multiple mineral deposit types to be realised within a single mineral system, thereby acknowledging the inherent natural variability among mineral deposits (Wyborn et al., 1994).

In this approach, the critical processes acting together to form mineral deposits are (Hronsky, 2004; Knox-Robinson and Wyborn, 1997; Kreuzer et al., 2008; Lord et al., 2001; McCuaig and Hronsky, 2000; McCuaig et al., 2010; Porwal and Kreuzer, 2010; Wyborn et al., 1994):

- Source: All geological processes required for extraction of necessary ore components (melts or fluids, metals and ligands) from crustal and/or mantle sources;
- Transport: All geological processes required for melt- or fluid-assisted transfer of ore components from sources to traps (i.e., effective, active melt or fluid pathways);

- Trap: All geological processes required to focus melt or fluid migration into channels that can accommodate metal deposition;
- Deposition: All geological processes required for extraction of metals from melts or fluids passing through the traps; and
- Preservation: All geological processes required to preserve the accumulated metals through time.

Whilst none of these processes can be directly observed or mapped, we can observe and map in our geoscience datasets the expressions of these processes (i.e., the targeting elements: McCuaig et al., 2010). The GIS environment is ideally suited for this task and for using this information to create derivative predictor maps, spatial maps that serve as spatial proxies for these mappable targeting criteria and, thus, for the critical ore-forming processes (McCuaig et al., 2010; Porwal and Kreuzer, 2010).

The mineral systems approach is essentially a probabilistic concept in that if the probability of occurrence of any of the critical processes becomes zero, then no deposit will be present (Kreuzer et al., 2008; Lord et al., 2001; McCuaig et al., 2010). By integrating mineral systems models into a probabilistic framework a prior probability of success can be calculated for discovery of a potentially economic mineral deposit in an area. This thinking has been applied to valuation of exploration programs (Lord et al., 2001), development of targeting decision and ranking tools (Kreuzer et al., 2008), economic risk analysis (Partington, 2010), and prospectivity analysis (e.g., González-Álvarez et al., 2010; Joly et al., 2012; Kreuzer et al., 2010; Porwal et al., 2010).

### 4.2. Porphyry Cu–Au mineral systems model

Porphyry Cu–Au deposits and the processes critical in their formation (Fig. 2, Table 1) were summarised in detail by Sillitoe (2000, 2010), Tosdal and Richards (2001), Candela and Piccoli (2005), and Seedorff et al. (2005). These summaries informed the mineral systems model outlined below.

#### 4.2.1. Source processes

Source processes critical to the formation of porphyry Cu–Au deposits in the Macquarie Arc would have most likely included (i) melt generation in the mantle below the arc due to melting of the subducted oceanic crust and the mantle wedge overlying the subducted slab, (ii) underplating of mantle-derived melts at the base of the crust and/or intrusion of these melts into the lower crust along zones of lithospheric weakness (i.e., major translithospheric structures), (iii) partial melting of the lower crust triggered by the arrival of these mantle-derived melts, (iv) formation of long-lived, deep crustal magma chambers ( $\geq 6$  km below earth's surface) that are episodically replenished and fractional crystallisation of the magma in these chambers, and (v) extraction of metals from mantle and/or crustal sources and partitioning of these metals into melts (Richards, 2003; Tosdal and Richards, 2001; Wilkinson, 2013).

#### 4.2.2. Transport processes

Transport processes critical to the formation of porphyry Cu–Au deposits in the Macquarie Arc would have most likely included (i) a change in plate motion or angle of subduction, promoting extension, dilational deformation and vertical permeability, (ii) magma escape from deep crustal magma chambers via apophyses, and (iii) emplacement of porphyritic intrusions and dyke swarms to within 1 to 4 km of the surface controlled by buoyancy forces and permeable (sub-)vertical conduits, in particular translithospheric, arc-parallel, strike-slip structures that served as a primary control on magma emplacement in many volcanic arcs (Richards, 2003; Wilkinson, 2013).

#### 4.2.3. Trap processes

Trap processes critical to the formation of porphyry Cu–Au deposits in the Macquarie Arc would have most likely included (i) stalling of

magma ascent, for example, due to reduction of magma pressure or supply, intersection of a physical barrier to magma ascent, or increasing magma viscosity as the melt cools to near-solidus temperatures, (ii) exsolution of volatile phases from the cooling magma and consequential volume expansion and wallrock alteration, and (iii) recurring fracturing and/or brecciation of enclosing, previously deformed country rocks driven by multiple intrusive events and magmatic-hydrothermal (e.g., volume expansion, overpressuring) and/or tectonic processes (e.g., dilational deformation) (Richards, 2003; Tosdal and Richards, 2001). Size and continuity of the resulting traps (i.e., interconnected fracture networks or breccia bodies that served as efficient fluid pathways) and development of sufficient permeability are important variables as they determine the size and continuity of any resulting orebody.

#### 4.2.4. Deposition processes

The metal deposition process critical to the formation of porphyry Cu–Au deposits in the Macquarie Arc was most likely triggered by cooling and depressurization of metal-bearing hydrothermal fluids that exsolved from the magma and by reaction of these fluids with surrounding reactive wall rocks. Discharge of these metal-bearing hydrothermal fluids upwards and/or outwards from the magmatic source would have been fracture-controlled with the fracture networks also facilitating outflow of the spent fluids (Richards, 2003; Wilkinson, 2013). The efficiency and duration of this process is what ultimately controls the grade and tonnage of any resulting orebody.

#### 4.2.5. Preservation processes

Porphyry Cu–Au deposits in the Macquarie Arc are commonly well preserved, in particular within low strain zones that recorded little post-Ordovician uplift such as the WNW–ESE-striking Lachlan Transverse Zone. Further evidence for widespread preservation within the Macquarie Arc of the “porphyry environment” includes (i) the occurrence of epithermal level systems that typically form in the upper kilometre of the Earth's crust, and (ii) the occurrence of volcanic centres, comagmatic with and intruded by Early Ordovician to Early Silurian porphyry complexes (Cooke et al., 2007; Glen et al., 2012). For the purpose of this study the assumption was made that porphyry Cu–Au deposits were relatively well protected from erosional processes everywhere within the Macquarie Arc.

## 5. Spatial and prospectivity analysis

### 5.1. Introduction

The study area (Fig. 1), which is defined by the Narromine, Dubbo, Forbes, Bathurst, Cootamundra, and Goulburn 1:250,000 scale map sheets (with a buffer of 20 km), was selected to match the area examined in a previous study of historic porphyry Cu–Au exploration activities and related expenditure that is summarised in Section 7.

Data collection and prospectivity analysis undertaken by Kenex Limited ([www.kenex.com.au](http://www.kenex.com.au)), on the other hand, were carried out over the entire New South Wales portion of the Lachlan Fold Belt, an area that is much larger than the study area. The benefits of undertaking the modelling at the belt-scale are that the analysis (i) covered as much of the permissive area for Late Ordovician to Early Silurian porphyry Cu–Au deposits as possible, (ii) encompassed more training data, and (iii) provided more realistic and holistic results representing the prospectivity of the study area as a function of belt-scale prospectivity and based on a porphyry Cu–Au mineral system model for the entire belt.

### 5.2. Weights of evidence (WofE) approach

Spatial analysis was carried out using the WofE approach in combination with the Spatial Data Modeller extension (Sawatzky et al., 2010) ([www.ige.unicamp.br/sdm/ArcSDM10](http://www.ige.unicamp.br/sdm/ArcSDM10)) for ESRI's ArcGIS software.

WofE is a data-driven Bayesian probability method for combining evidence in support of a hypothesis. The method was originally developed for medical diagnosis (Spiegelhalter, 1986) but subsequently adopted for mineral prospectivity modelling with GIS (Bonham-Carter, 1994; Bonham-Carter et al., 1989). Deng (2009) described WofE modelling as a method that relates the presence of mineral deposits to a number of binary predictor maps of geological features. These predictor maps (i.e., evidence maps reflecting mappable criteria of a particular mineral system) are used as inputs in and are combined to generate a map of estimated posterior probabilities of occurrence of mineral deposits or mineral prospectivity map (Deng, 2009; Harris et al., 2001).

WofE modelling comprises five stages: (i) Estimation of prior probability (i.e., the probability of a mineral occurrence existing in a predetermined area computed before considering or collecting any additional information); (ii) determination of weighting coefficients; (iii) calculation of posterior probability (i.e., the probability of a mineral occurrence existing in a predetermined area computed after determination of weights and introducing additional information), (iv) testing for conditional independence and (v) model validation (Bonham-Carter, 1994; Bonham-Carter and Agterberg, 1990; Bonham-Carter et al., 1989; Lindsay et al., 2014; Raines et al., 2000).

Employing Bayesian statistics, the WofE approach is used to (i) compute the spatial relationship between the predictor maps and a set of known mineral occurrences (i.e., the training data), and (ii) assign each predictor map feature class a pair of weights,  $W^+$  and  $W^-$ . A positive  $W^+$  value indicates a positive association between the training data and predictor map feature, whilst a negative  $W^+$  value indicates the opposite. A non-zero  $W^-$  value indicates that a spatial relationship exists between the training data and the absence of the predictor map feature, with positive values indicating a positive relationship and negative values indicating a negative relationship. If there is no spatial relationship between the training data and a particular predictor map feature, then  $W^+ = W^- = 0$ . The contrast value  $C$  (where  $C = W^+ - W^-$ ) reflects the degree of spatial relationship between the predictor map and the training data; as such, the larger the  $C$  value the stronger the spatial relationship. The standard deviations of the pair of weights and contrast values are also calculated ( $W_s$  and  $C_s$ ), providing a studentised value of the contrast (StudC; Table 1). StudC refers to the ratio of the contrast  $C$  to the standard deviation of the contrast  $C_s$  and gives an informal test of the hypothesis that  $C = 0$ . Therefore, a StudC value greater than 1.5 (or smaller than  $-1.5$ ) infers a true, strong positive (or negative) correlation and a StudC value greater than 0.5 but less than 1.5 (or less than  $-0.5$  but more than  $-1.5$ ) infers a true but weak positive (or negative) correlation. One of the limitations of the WofE approach is that it assumes conditional independence between the predictor maps. This assumption is commonly violated when producing a prospectivity map based on posterior probabilities from geological data and so potentially introduces an element of bias (Harris et al., 2001).

Being a data-driven approach, WofE modelling was ideally suited for this spatial analysis of a study area that is data-rich not only with respect to mineral occurrences that can be used as training data but also with respect to geological, geochemical and geophysical datasets offering uniform coverage of the study area.

### 5.3. Study area GIS

Most digital data used in this study were open-file and sourced from either the Geological Survey of New South Wales ([www.resources.nsw.gov.au/geological](http://www.resources.nsw.gov.au/geological)); Eastern Lachlan Orogen Geoscience Data: [www.shop.nsw.gov.au/proddetails.jsp?publication=6866](http://www.shop.nsw.gov.au/proddetails.jsp?publication=6866)) or Geoscience Australia ([www.ga.gov.au](http://www.ga.gov.au)). Key data used in this study are:

- Mineral occurrences, including the training data (Table 2): Attributed vector data, extracted from a proprietary mineral occurrence database

owned by Kenex Limited, providing information about or descriptions of commodity type, deposit size and production, mineralisation style and ore minerals;

- **Geology:** Attributed vector data providing information about or descriptions of unit name, rock type and class, lithology and geological age;
- **Faults:** Partly attributed vector data only providing incomplete information about or descriptions of fault types and senses of movement (available for only 245, or 6%, of the 3807 faults and fault segments in the study area) and no information about fault age, thereby severely limiting the detail of analysis possible;
- **Geochemistry:** Attributed vector data capturing locations and geochemical assay results (e.g., Au, Cu) of stream sediment and rock chip samples and drill holes; and
- **Geophysics:** High resolution (50 m grid cell size) TMI and 1VD RTP airborne magnetic raster data; and moderate resolution (100 m grid cell size) airborne K, Th and U radiometric data.

Examples of important digital datasets not utilised in the spatial analysis are:

- **Folds:** Information about folds is biased toward the relatively data-rich Dubbo and Bathurst 1:250,000 scale map sheet areas whereas the other map sheets, in particular Cootamundra, are relatively data-poor with respect to fold axial traces,
- **Soils:** Open-file soil sampling data are scarce ( $n = 325$ ) and of incomplete, irregular coverage, and only 25% ( $n = 82$ ) of these samples have

been assayed for Au,

- **Gravity:** Their low resolution (500 m grid cell size) makes the gravity data unsuitable for use in a prospectivity analysis.
- **Radiometrics:** Their low penetration depth and incomplete coverage makes the of the airborne gamma-ray spectrometer data (Th, K and U) unsuitable for use in a prospectivity analysis.

#### 5.4. Predictor maps

The predictor maps outlined below are based on predictive evidence extracted from spatial datasets using the porphyry Cu–Au mineral systems model described in Section 4. The descriptions below consider only those predictor maps that were used in the prospectivity model (Table 1). Appendix 1 provides a summary of the more than 80 predictor maps produced in this study.

##### 5.4.1. Predictor maps for source processes

None of the processes of energy and mass flux described in the porphyry Cu–Au system model can be mapped but their expressions in our geoscience datasets can. Mappable geological features indicative of these processes having operated in the Macquarie Arc are (i) the presence of large volumes of arc-related volcanic and intrusive rocks contained in four, several 100 km-long belts that formed within a much more extensive convergent margin system spanning the entire proto-Pacific margin of Gondwanaland, (ii) its 40 + million year history of volcanic and intrusive activity, (iii) Ordovician magmatic zircons with

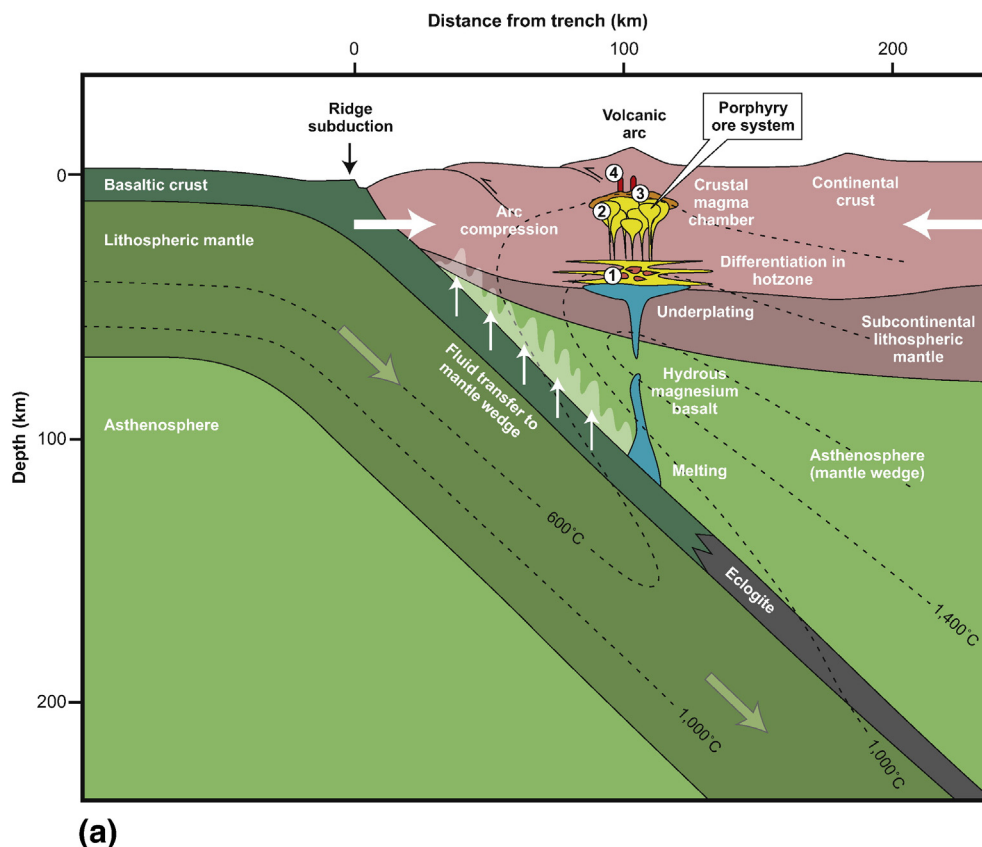
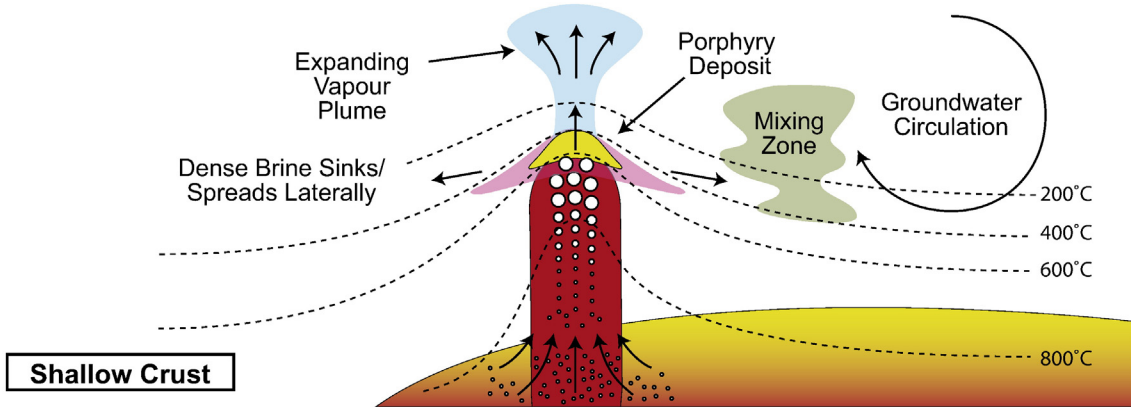


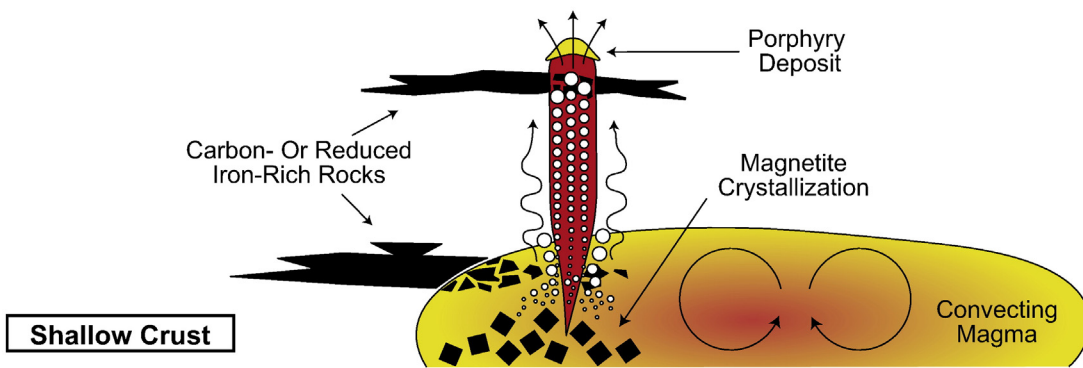
**Fig. 2.** (a) Suprasubduction zone setting for the formation of porphyry Cu–Au deposits. The four environments where key processes operate are labelled (b) to (e) with these labels corresponding to Fig. 2b–e, respectively. (b) Mafic magma underplates the base of the continental crust, triggering melting and assimilation of crustal rocks. In a compressional tectonic regime mafic magmas get trapped in deep crustal sills where they evolve to intermediate-to-felsic compositions. Cycles of addition of fresh mafic magma and fractional crystallisation increase the content of volatiles and metals to generate fertile magmas. (c) Sulphide saturation of intermediate-to-felsic magmas leads to stripping of metals into a sulphide-melt phase. If the sulphide is later remelted by mafic intrusions or dissolved by exsolving volatiles then a highly enriched melt or volatile phase will be generated. (d) Melt reduction triggered by magnetite crystallization, or assimilation of reducing crustal rocks, promotes the partitioning of reduced sulphur species into volatiles exsolving from the melt (in response to “first boiling” and “second boiling” processes; cf. Cline, 2003), efficiently extracting Cu, Au and other sulphur-complexed metals to produce highly enriched ore fluids. (e) Efficient focusing of hydrothermal fluid flow and cooling across a steep thermal gradient, combined with expansion of an ascending single-phase fluid, could force metal deposition in a limited rock volume, creating a porphyry Cu–Au deposit. Figure modified from Winter (2001) and Wilkinson (2013).



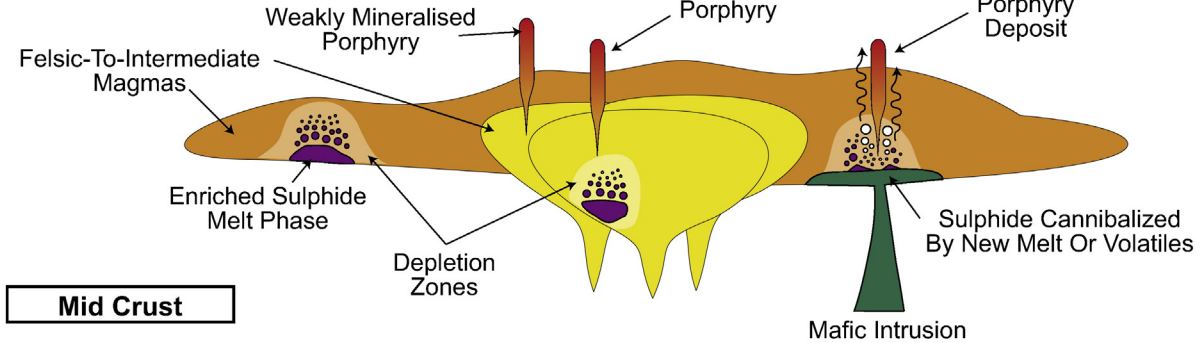
**(e) Efficient precipitation at the deposit trap site (trigger 4).**



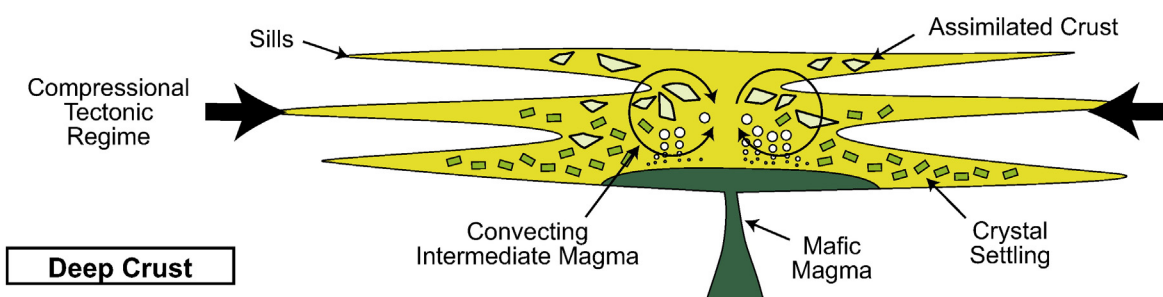
**(d) Melt reduction and enhanced metal partitioning (trigger 3).**



**(c) Magmatic sulphide saturation (trigger 2).**



**(b) Cyclic fractionation in deep crustal magma chambers (trigger 1).**



Progressively Shallower Crustal Level And Larger Scale

Fig. 2 (continued).

positive  $\epsilon_{\text{Hf}}$  values, indicating derivation from unevolved mantle-derived magmas, consistent with formation in an intraoceanic island arc, and (iv) its significant Cu–Au endowment contained in various porphyry Cu–Au and related mineral occurrences and deposits (Cooke et al., 2007; Glen et al., 2007b; Glen et al., 2011).

Proxies (also referred to as mappable criteria: Wyborn et al., 1994; or mappable targeting criteria: McCuaig et al., 2010) for source processes are limited, in particular those that have uniform coverage over the study area and, thus, are relatively unbiased (Porwal and Kreuzer, 2010). The most suitable and powerful of these are lithological and stratigraphic information, readily available for the entire study area from attributed digital geological maps.

Porphyry Cu–Au deposits in the Macquarie Arc are contained either within Ordovician to Silurian intrusive complexes or in rocks adjacent to such complexes. Roof pendants and adjacent rocks are often volcanic and part of volcanic centres that were comagmatic with the mineralised porphyries (Cooke et al., 2007). On the whole, these igneous rocks are probably the only uniform proxy for the Ordovician to Silurian arc-related magmatism and the processes that generated the melts and ultimately the porphyry Cu–Au deposits. As such, occurrence of and proximity to felsic to intermediate intrusive and volcanic rocks of Ordovician to Silurian age (Fig. 3a) served as the key evidence map for the source aspect of the mineral systems approach to prospectivity modelling (Table 1).

#### 5.4.2. Predictor maps for transport processes

Geological features indicative of the transport processes outlined above having operated in the Macquarie Arc include but are not limited to (i) sedimentary sequences of Llandovery age that were deposited in extensional or transtensional basins, reflecting arc extension and relaxation (possibly as a result of subduction zone rollback) at the same time as porphyry Cu–Au mineralisation and, (ii) high-level intrusive porphyries that were emplaced episodically into the Macquarie Arc between Early Ordovician (c. 481 Ma) and earliest Silurian (c. 437 Ma), and (iii) arc-parallel and arc-transverse faults and fault intersections that, in the Macquarie Arc, are spatially and most likely genetically associated with porphyry Cu–Au mineralisation (Cooke et al., 2007; Glen et al., 2007a,b; Glen et al., 2011; Tosdal and Richards, 2001).

Llandovery age basin sequences are a good proxy for the tectonic regime at the time of porphyry Cu–Au mineralisation but they are of little use as a vector towards mineralised porphyries. The occurrence and distribution of high-level intrusive porphyries is an excellent guide but not conditionally independent from some of the source processes outlined above. As such, structural data are the only reliable and readily available proxies also satisfying the critical requirement of having uniform coverage of the study area. As summarised in Table 1, suitable proxies for

dilational deformation and vertical permeability are medium to high fault density (Fig. 3b) and fault orientation, in particular N–S (arc parallel structures) and NW–SE (arc transverse structures) (Fig. 3c). Unfortunately, the New South Wales GIS fault database contains no information regarding fault ages and only discriminates to a minor extent between thrust and non-thrust faults.

#### 5.4.3. Predictor maps for trap processes

There are few proxies for the above trap processes apart from lithology and structure as evident in the currently exposed upper crustal architecture of the Macquarie Arc. Zones of dilation, which offer high-permeability pathways for the focused ascent of magma from lower crustal zones and a perfect environment for development of aerially and volumetrically extensive fracture networks in upper crustal zones, may be represented by fault intersections or fault bends (Richards, 2003; Tosdal and Richards, 2001). Competency contrasts among lithological units may give rise to local zones of dilation and permeability, focusing fluid flow at or close to lithological contacts. In addition, lithology may play a role in enhancing ore grade with impermeable rock units such as limestone preventing fluid escape and metal dispersion (e.g., at Grasberg, Indonesia) or providing a reactive host for high-grade skarns (Wilkinson, 2013).

The key predictors selected for the prospectivity modelling were proximity to calcareous rocks (Fig. 3d), competency contrasts among lithological units (Fig. 3d), and to fault bends and fault intersections (Fig. 3e). Total magnetic intensity (TMI) grids and derivative grids were used to identify magnetic highs (Fig. 3f) that captured the maximum number of training data and may reflect magnetite- or pyrrhotite-rich porphyry-related alteration zones (Table 1).

#### 5.4.4. Predictor maps for deposition processes

Evidence for the above deposition processes having operated in the Macquarie Arc includes but is not limited to (i) occurrence of porphyry Cu–Au deposits comprising mineralised stockwork-like or sheeted quartz vein arrays, disseminations and/or breccia associated with potassic alteration assemblages, and (ii) analytical data demonstrating the magmatic origin of the hydrothermal fluids (i.e., hypersaline brines  $\pm$  low-density vapours) that formed the porphyry Cu–Au deposits (Cooke et al., 2007). An additional proxy for depositional processes having occurred is (iii) the relative enrichment of rocks, soils and stream sediments near porphyry Cu–Au deposits in a range of pathfinder elements such as Au, Ag, Cu, As, Mo, Pb, Zn, Sb and Hg (Table 3).

As illustrated in Table 1, the key predictor maps selected for the prospectivity modelling based on data coverage and statistical and spatial analyses were anomalous Au in stream sediments (Fig. 3g), anomalous Cu and Ag in rock chips and drill chips/core (Fig. 3h). Additional

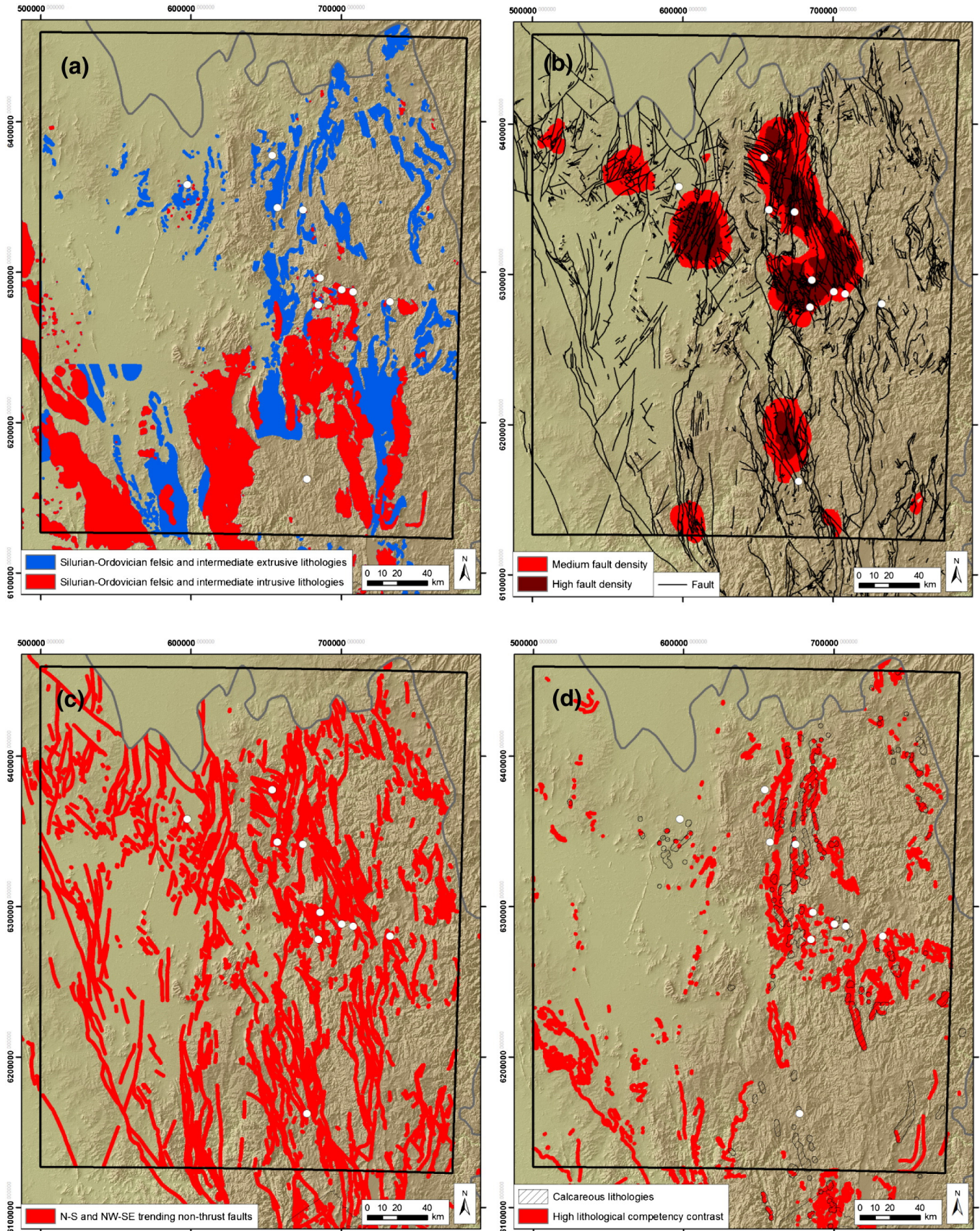
**Table 2**

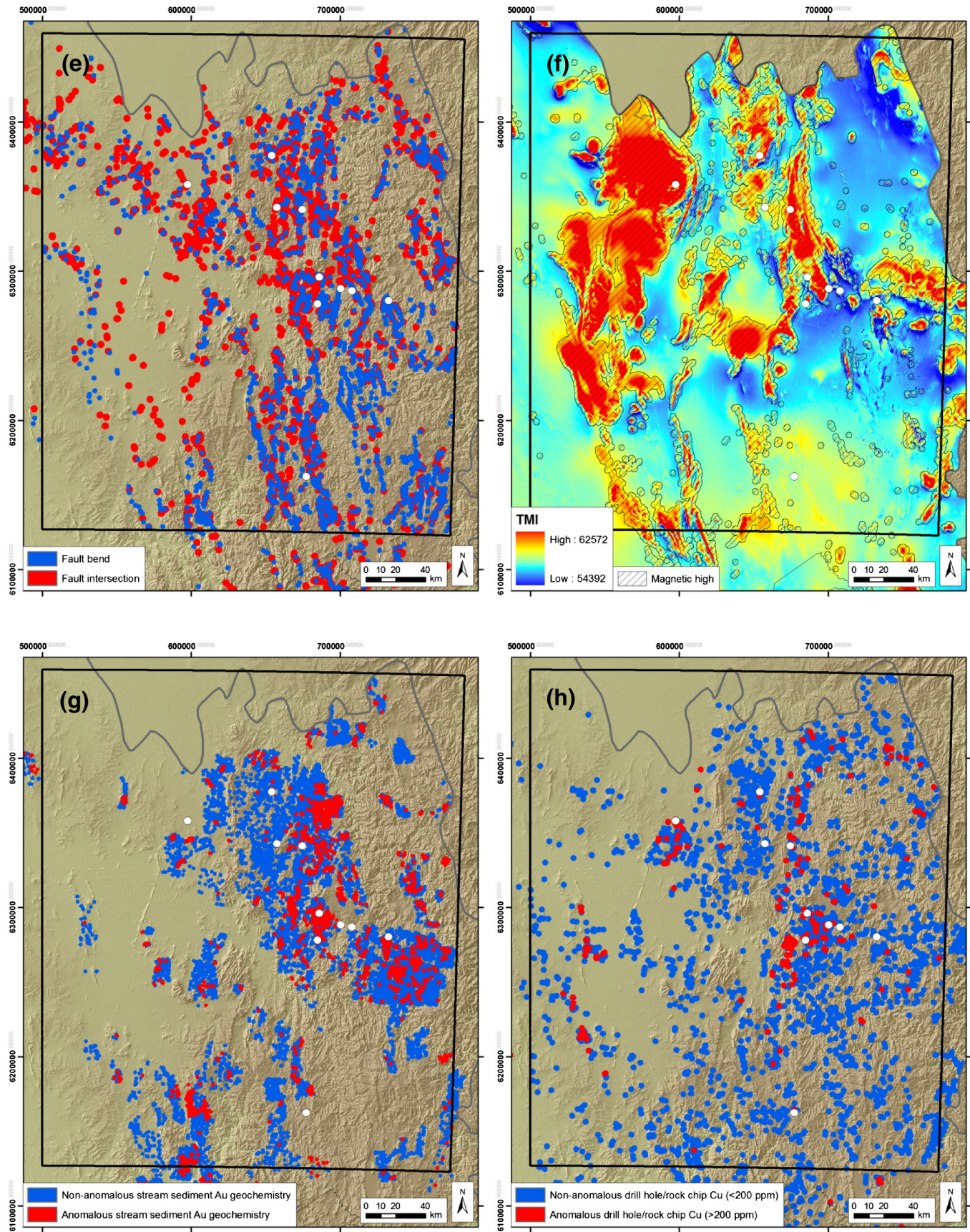
Ordovician to Early Silurian porphyry Cu–Au and related skarn deposits used as training data for the porphyry Cu–Au prospectivity model. Data sources: Geological Survey of New South Wales (2006); Thomas and Moorehead (2011); www.riotinto.com.

Deposit name	Mineral deposit type	Host rocks	Production
Cadia Hill	Porphyry Cu–Au	Quartz monzonite porphyry	233 t Au; 338,000 t Cu (as at 2010)
Northparkes	Porphyry Cu–Au	Trachyandesite, trachyte, volcanoclastic rock, quartz monzonite porphyry	30.6 t Au; 715,000 t Cu (as at 2009)
Doradilla	Skarn Sn–Cu	Sandstone	20 t Cu
Yeoval	Porphyry Cu–Mo	Granodiorite	10 kg Cu
Browns Creek	Skarn Cu–Au	Limestone near contact with granodiorite and basalt	6.5 t Ag; 8.4 t Au; 6062 t Cu
Blayney	Skarn Cu	Basalt	867.7 t Cu
Sheahan-Grants	Skarn Cu–Au	Siltstone near contact with monzodiorite	5.8 t Au
Copper Hill	Porphyry Cu–Au	Dacite	0.1 kg Au
Delayneys Dyke	Skarn Cu–Au	Sandstone–granite contact	1.3 kg Ag; 65 kg Au
Red Hill	Skarn Cu–Au	Tuff and minor volcanic rocks	1.1 kg Au
Ardlethan	Porphyry Sn–Cu	Granite–quartzite contact	5872 t Sn
Balmoral	Skarn Cu–Zn	Marble within volcanoclastic unit	1.4 t Cu
Kyloe	Porphyry Cu–Au	Granite–sandstone contact	3674 t Cu

important predictors include Au occurrences (Fig. 3i), areas of high magnetic gradient between high and low magnetic values given that the location of porphyry Cu–Au deposits often coincides with magnetic

slopes rather than intense magnetic highs or lows (Fig. 3j), and areas of low magnetic values that may indicate zones of magnetite destruction in rocks proximal to porphyry Cu–Au deposits.





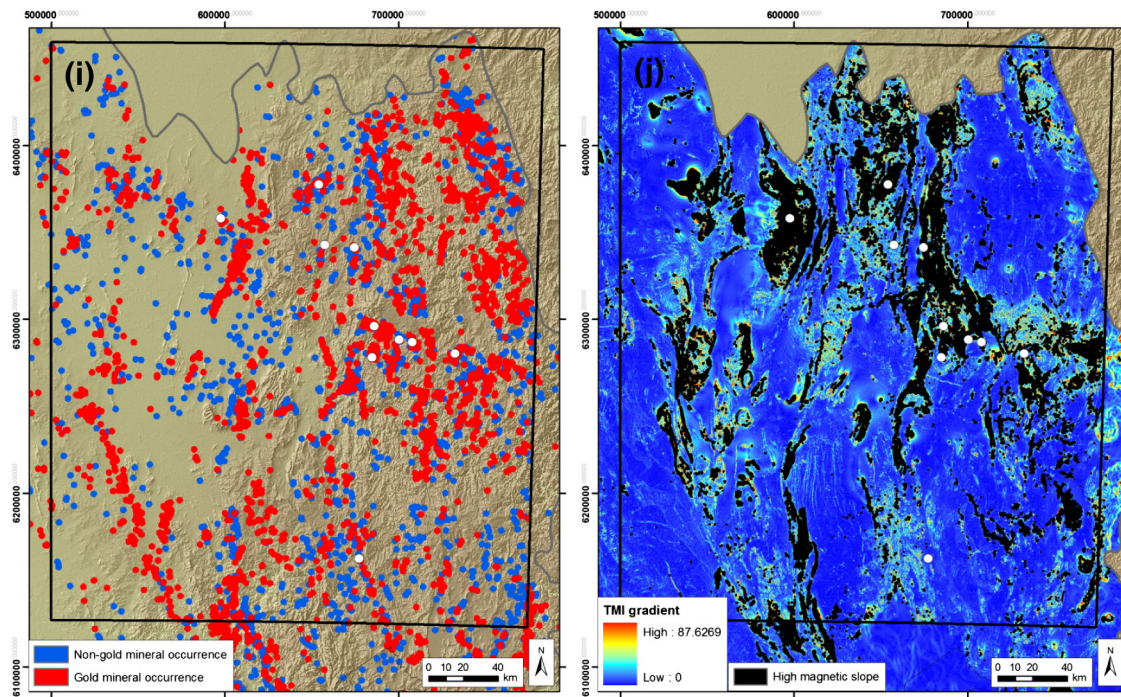


**Fig. 3.** Predictor maps of the porphyry Cu–Au WofE model. (a) Proximity to felsic to intermediate intrusive and volcanic rocks of Ordovician to Early Silurian age. A prominent feature in this predictor map is the abrupt termination of prospective geology within the Cootamundra (SI/55-11) 1:250,000 scale map sheet (in the SW corner of the GEMOC study area: Fig. 1) against the boundary with the Forbes (SI/55-7) 1:250,000 scale map sheet to the north. The abrupt termination can be explained with the respective map authors having interpreted the geology in a different manner; in this case as mainly bedrock on the Cootamundra sheet and as mainly cover on the adjacent Forbes sheet. Issues such as this introduce bias to a prospectivity analysis whilst attempts to fix such an issue without appropriate area knowledge may lead to introduction of significant uncertainty and additional bias. (b) Proximity to areas of medium and high fault density. (c) Proximity to N–S (arc parallel) and NW–SE (arc transverse) striking faults. (d) Proximity to calcareous rocks and domains of high lithological competency contrast. (e) Proximity to fault bends and fault intersections. (f) Proximity to magnetic highs. (g) Proximity to anomalous Au in stream sediments. (h) Proximity to anomalous Cu in rock chips and drill chips/core. (i) Proximity to Au occurrences. (j) Proximity to areas of high magnetic slope. Key to symbols: White circles = Porphyry Cu–Au training data; black outline = GEMOC study area; grey outline = Prospectivity study area.

### 5.5. Spatial analysis

The first step in the spatial analysis was the generation of a 50 by 50 m grid covering the entire Lachlan Fold Belt in New South Wales. This grid size represents the minimum resolution at which the data should be viewed at.

The second step was the collation of a set of training data. In this step, porphyry Cu–Au and related skarn occurrences were extracted from Kenex Limited's in-house Lachlan Fold Belt mineral occurrence database, which is mainly based on open-file data held by the Geological Survey of New South Wales. Following data validation and quality assurance and quality control, a training dataset ( $n = 13$ ) was extracted containing a selection of mined porphyry Cu–Au and related skarn deposits for which production figures are available (Table 2).

A unit cell grid of  $2 \text{ km}^2$  was used for the spatial statistical calculations representing the average area covered by porphyry Cu–Au deposits. By multiplying the unit cell value by the number of training data and dividing it by the total area of the prospectivity study (Fig. 1), a prior probability can be calculated that represents the probability of one porphyry Cu–Au deposit existing within any of the  $2 \text{ km}^2$  unit cells given no additional information (i.e., prior probability =  $2 \times 13:199,300 \text{ km} = 0.000131$ ; chance = 0.01%; odds = 1 in 10,000). The prior probability of a porphyry Cu–Au deposit existing within a randomly chosen unit cell of the much smaller GEMOC study area is 0.000216 (chance = c. 0.02%; odds = 1 in 5000).

#### 5.5.1. Spatial analysis of lithological data

As discussed above, lithology is one of the few proxies for source processes critical in the formation of porphyry Cu–Au deposits. In addition, lithological features can be important ingredients in trap processes, for example, (i) impermeable rock units such as limestone may play a

role in enhancing ore grade by preventing fluid escape and metal dispersion or providing a reactive host for high-grade skarns, whilst (ii) competency contrasts among lithological units may give rise to local zones of dilation and permeability, focusing fluid flow at or close to lithological contacts (Wilkinson, 2013).

Given the spatial, temporal and genetic association in the Macquarie Arc between porphyry Cu–Au deposits and intermediate intrusive complexes, it was not surprising to see a strong spatial association between the training data and intermediate intrusive lithologies (C value of 2.9; studC value of 2.8). Expanding the data evaluation to include geological age, the group of felsic to intermediate intrusive rocks of Ordovician to Silurian age recorded the strongest spatial correlation (C = 1.6; studC = 2.9). Felsic to intermediate extrusive rocks of Ordovician to Silurian age were also tested but recorded a weak spatial correlation (C = 0.8; studC = 1.1). Despite the weak spatial association, this lithological group was included in the prospectivity model. The reason for including the felsic to intermediate extrusive rocks of Ordovician to Silurian age is that they constitute an important ingredient of the porphyry Cu–Au mineral system model in that some of these rock packages represent the tops of intrusive centres at depth. Based on this rationale, both lithological groups were combined into a single multi-class predictor map (Fig. 3a, Table 1).

As outlined above and considering the Cadia district skarns (cf. Forster, 2009; Forster et al., 2004) example, the strong spatial association between Early Silurian and older calcareous rocks and the training data (C = 2.7, studC = 4.0) is best explained by their role as permeable fluid pathways and chemical and physical trap for Cu–Au mineralisation.

Competency contrasts among different lithological units are an important ingredient in trap processes. Creation of a relevant predictor map required that each rock type be assigned a generic competency value on a scale from one to 10, with one being the least and 10 being

**Table 3a**  
Summary of stream sediment assay statistics.

Element	Count	Max	Median	SD	70PI	80PI	90PI	98PI	ioGAS Threshold
Ag (ppb)	27,418	400,000.0	25.0	6516.0	500.0	1000.0	1000.0	10,700.0	500 ppb
As (ppm)	38,317	12,700.0	4.7	92.1	8.0	11.7	20.0	70.0	80 ppm
Au (ppb) <sup>a</sup>	33,647	373.2	0.3	3.6	1.0	1.5	2.6	6.2	2.62 units
Bi (ppm)	30,212	890.0	0.025	17.4	0.2	0.4	10.0	30.0	
Co (ppm)	13,764	1700.0	11.0	28.8	18.0	20.4	30.0	55.0	
Cu (ppm)	143,708	27,500.0	15.0	100.1	24.0	32.0	55.0	110.0	95 ppm
Mn (ppm)	16,863	42,400.0	380.0	770.3	640.0	850.0	1200.0	2277.6	640 ppm
Mo (ppm)	33,548	950.0	0.1	13.8	1.3	2.0	5.0	15.0	5 ppm
Pb (ppm)	138,780	31,000.0	20.0	145.9	26.0	30.0	40.0	82.0	60 ppm
Sb (ppm)	14,746	1414.0	0.3	15.3	0.8	1.7	5.0	12.9	
Se (ppm)	512	1.0	1.0	–	1.0	1.0	1.0	1.0	
Sr (ppm)	512	331.0	47.0	69.9	72.0	114.0	200.8	272.1	
Te (ppm)	6592	90.0	0.025	1.3	0.025	0.025	0.025	0.2	
W (ppm)	20,094	8000.0	0.5	231.2	0.5	5.0	10.0	555.0	10 ppm
Zn (ppm)	139,564	35,900.0	45.0	137.9	60.0	70.0	90.0	185.0	105 ppm

<sup>a</sup> Levelled.**Table 3b**  
Summary of rock chip and drill hole assay statistics.

Element	Count	Max	Median	SD	70PI	80PI	90PI	98PI	ioGAS Threshold
Ag (ppm)	4804	300.00	0.00005	8.08	0.10	1.00	2.00	5.00	1 ppm
As (ppm)	7779	14,324.00	2.00	179.73	4.50	7.50	15.00	78.44	122 ppm
Au (ppm)	4086	69.50	0.05	3.65	0.09	0.40	2.80	11.82	0.12 ppm
Bi (ppm)	4828	1215.00	0.00005	34.00	0.20	2.00	8.58	52.00	1 ppm
Co (ppm)	4501	273.00	13.00	23.28	21.00	31.00	46.00	83.00	16 ppm
Cu (ppm)	11,259	99,999.00	17.00	1270.78	45.00	76.10	157.10	754.84	200 ppm
Mn (ppm)	2505	2850.00	535.00	400.48	720.00	911.00	1218.00	1644.60	800 ppm
Mo (ppm)	3587	590.00	0.80	22.56	1.90	3.00	4.50	22.56	45 ppm
Pb (ppm)	11,397	55,000.00	11.00	699.40	18.00	24.00	32.00	144.08	90 ppm
Sb (ppm)	2022	167.00	0.30	6.54	0.70	1.53	4.49	11.00	0.8 ppm
Se (ppm)	521	830.00	0.00001	36.39	0.00001	0.00001	0.00001	3.60	2 ppm
Sr (ppm)	8875	3966.00	221.00	365.93	426.80	600.08	840.90	1363.00	1400 ppm
Te (ppm)	220	39.60	0.00001	3.01	0.00001	0.00001	0.07	4.32	0.06 ppm
W (ppm)	1432	2461.00	1.86	108.79	6.00	10.00	16.00	205.38	18 ppm
Zn (ppm)	11,240	91,000.00	56.00	1222.82	77.00	90.00	113.00	284.22	175 ppm

the most competent. Where differences in competency contrast were identified between adjoining lithological units their lines of contact were extracted and their spatial correlation tested against the training data. The strongest spatial correlation was recorded for differences in competency contrast greater than three ( $C = 1.8$ ;  $\text{stud}C = 3.24$ ).

### 5.5.2. Spatial analysis of structural data

Structure is an essential ingredient of the porphyry Cu–Au mineral system model; in particular faults or interconnected fault networks (i.e., areas of high fault/fracture density: cf. [Tripp and Vearncombe, 2004](#)) that may act as (i) pathways for melt and fluid migration, (ii) sites for fluid focussing or fluid mixing, and (iii) loci for mineral deposition. The latter is commonly localised at fault splays, fault bends, fault jogs and fault intersections given the high gradients in permeability and hydraulic head centred upon these structural settings (cf. [Cox, 1999](#); [Cox et al., 2001](#)).

Prior to evaluating the spatial association between faults and the training data the following steps were taken to make the digital fault data more amenable to spatial modelling and to extract essential derivative information:

- The highly segmented fault data were revised in that contiguous fault segments of similar orientation were joined to create a more coherent fault map;
- Thrust faults (where attributed as such) were removed from the data because of the demonstrated preferred spatial association between porphyry Cu–Au deposits and extensional or transtensional structures;

- Strike orientations were assigned to each fault segment using Map Info Spatial Data Modeller (MI-SDM; [www.avantra.com.au/mi-sdm.htm](http://www.avantra.com.au/mi-sdm.htm));
- Faults were attributed with length in kilometres;
- Point data were created for fault intersections, fault bends, fault jogs and fault splays using MI-SDM; and
- A multi-class fault density predictor map was created by gridding the density of non-thrust faults using the kernel method and a 2000 m search radius in ArcMap Spatial Analyst using two cut-offs for the top 28% and the top 43% of a sliding density scale.

A major shortcoming of the fault data as provided by the Geological Survey of New South Wales is the incomplete attribution of these data. For example, there are approximately 5450 faults in the Lachlan Fold Belt database. Of these 550 are classified as reverse or thrust faults whilst the remaining 4900 faults are attributed as ‘unknown’ type or not attributed at all. In addition, the fault data lack information about many additional important features such as fault age (minimum ages were added to the database by Kenex Limited) or dip direction. The main implications of incomplete or missing information are (i) potential introduction of error and bias, and (ii) any spatial model being less precise than what it could be.

The spatial relationship between the faults and the training data was assessed for both the entire fault data and for subdivisions of this dataset grouped by fault orientation, length and type ([Table 1](#)). The most significant spatial association observed in this analysis is that between the training data and the groups of N–S and NW–SE-striking faults buffered by 1300 m ( $C = 2.5$ ;  $\text{stud}C = 3.7$ ). In terms of fault intersections, fault

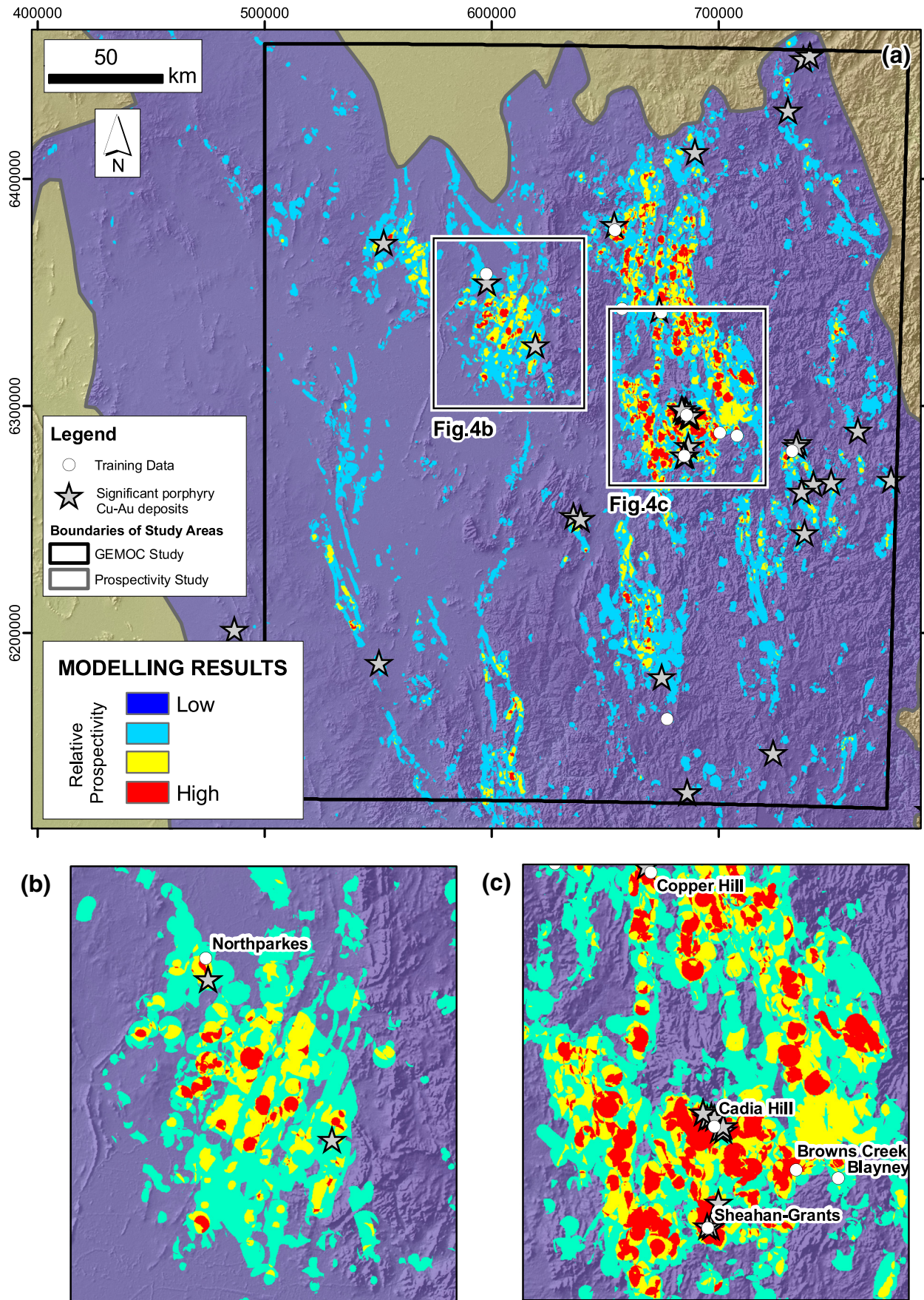


**Fig. 4.** Weights of evidence (WofE) based porphyry Cu–Au prospectivity model. Prospective areas were classified using natural breaks and range from relatively low (blue colours) to high (red colours) prospectivity. The remaining area is below the prior probability and considered unprospective for porphyry Cu–Au systems. (a) WofE model clipped to the GEMOC study area shown in Fig. 1. (b) Zoom-in view of the Cadia District. Inset boundary shown in panel a. (c) Zoom-in view of the Northparkes District. Inset boundary shown in panel a.

bends, fault jogs and fault splays, strong spatial correlations with the training data were recorded for the fault intersections ( $C = 2.4$ ;  $\text{studC} = 4.1$ ) and fault bends ( $C = 2.4$ ;  $\text{studC} = 4.2$ ). In addition, areas of high fault density ( $C = 3.3$ ;  $\text{studC} = 5.7$ ) and medium fault density ( $C = 1.6$ ;  $\text{studC} = 2.1$ ) have strong to moderate correlations with the training data, respectively.

### 5.5.3. Spatial analysis of geochemical data

Geochemical predictor maps were created based on relevant porphyry pathfinder elements, including Ag, As, Au, Bi, Co, Cu, Mn, Mo, Pb, Sb, W, and Zn. The ioGAS software ([www.iogas.net](http://www.iogas.net)) was used to format the drill hole, rock and stream sediment data and produce probability plots for determining anomaly thresholds for each of the pathfinder elements (Table 3).

Predictor maps were created for all stream sediment pathfinder elements. As a first step and to account for inconsistencies between the different assay methods, the Au-in-stream sediment data had to be levelled by assay method. The geochemical predictor maps for the pathfinder elements were created by buffering around the stream sediment sampling locations, thereby maximising the spatial correlation between the training data and the anomalous, non-anomalous and missing assay values for each sample location. The resulting geochemical predictor maps that correlate best with the training data are Ag ( $C = 1.9$ ;  $\text{studC} = 3.3$ ), Cu ( $C = 2.3$ ;  $\text{studC} = 3.1$ ), Au ( $C = 3.0$ ;  $\text{studC} = 2.8$ ) and Bi ( $C = 3.2$ ;  $\text{studC} = 4.9$ ).

Rock chip and drill hole assay data were combined in binary predictor maps showing anomalous areas, non-anomalous areas and areas of missing data for each pathfinder element. The resulting geochemical predictor maps that correlate best with the training data are Ag ( $C = 2.1$ ;  $\text{studC} = 1.8$ ), As ( $C = 3.3$ ;  $\text{studC} = 3.9$ ) and Cu ( $C = 3.8$ ;  $\text{studC} = 4.6$ ) (Table 1).

### 5.5.4. Spatial analysis of geophysical data

Airborne total magnetic intensity (TMI) data covering the Lachlan Fold Belt were analysed for magnetic lows, magnetic highs and strong magnetic gradients using ArcGIS 9.3. Magnetic lows, in particular when linear or circular, may represent areas of hydrothermal alteration where primary magnetite in the country rock was “destroyed” by interaction of these rocks with oxidising hydrothermal fluids. The reasonable spatial correlation between magnetic lows and the training data ( $C = 2.0$ ;  $\text{studC} = 3.5$ ) may be taken as corroboration of this proposition. Magnetic highs, on the other hand, can represent highly magnetic rocks or areas of hydrothermal magnetite alteration. Given the latter, it is not surprising that there is a good correlation between magnetic highs and the training data ( $C = 2.4$ ;  $\text{studC} = 3.7$ ). Strong magnetic gradients (Fig. 3j), which may represent areas of lithological contrast that have the capacity to localise deformation, fluid flow and associated ore deposition, exhibit a significant spatial correlation with the training data ( $C = 2.6$ ;  $\text{studC} = 4.5$ ).

## 6. Prospectivity modelling

A WofE-based prospectivity model (Fig. 4) was created using the predictor maps that represent all stages of the porphyry Cu–Au mineral system model. Table 1 provides a list of the predictor maps used to produce the final prospectivity map. For a predictor map to be incorporated in the modelling it had to meet the following criteria:

- Coverage of the modelled area (i.e., the Lachlan Fold Belt in New South Wales) had to be as complete and as uniform as possible;
- The spatial association with the training data had to be significant (i.e.,  $C > 1.0$ ;  $\text{StudC} > 1.5$ );
- Where possible, duplication of predictive map patterns had to be minimal as to avoid problems with conditional dependence.

The predictive capacity of the WofE-derived posterior probability model was tested statistically by plotting a success rate curve based

on the training data and an efficiency of prediction curve based on all other porphyry Cu–Au occurrences (Fig. 5). These site data were plotted cumulatively from high to low posterior probability against the cumulative area accumulated from high to low model posterior probability. The sum of the area under the efficiency curve provides a useful measure of model performance that improves as the efficiency percentage value approaches 100%. Values greater than 50% indicate statistically valid predictive efficiency. The curve for the training data in this model gave a success rate value of 99.9% and the curve for the mineral occurrence data gave an efficiency of prediction value of 87.6%. Both measures confirm that the model has a high predictive efficiency that is statistically valid not only for the training data but also for all other known porphyry Cu–Au occurrences in the Lachlan Fold Belt.

The Agterberg–Cheng test of conditional independence (Agterberg and Cheng, 2002) gave a conditional independence ratio of 100%, confirming that conditional independence is a significant problem in the model. The consequence of significant conditional dependence between predictor patterns is upward biasing of the posterior probabilities associated with geological, geochemical or geophysical characteristics that resemble each other, ultimately resulting in an overestimation of mineral prospectivity. This upward bias is a common issue in the application WofE approach (e.g., Agterberg, 2011; Schmitt, 2010) that, if possible, should be avoided. However, it is a problem that has little impact on the overall result if the numerical values derived from WofE modelling are being used in a relative rather than an absolute sense (cf. Lindsay et al., 2014). Given conditional dependence, the modelling results should be viewed as a relative measure of favourability. Despite this issue, the posterior probability values derived from the WofE model provide an effective means for rank-order analysis and highlighting areas where porphyry-type Cu–Au mineralisation may be present.

A further test of the rank-order assumption that area evaluation by relative rankings is valid is to examine the shape of the success rate curve, with a continuously decreasing slope area is accumulated indicating validity of the hypothesis whilst a sigmoidal shape indicates violation of the hypothesis. Within reasonable bounds, the success rate curve for this model is continuously decreasing as area is accumulated, validating the rank-order hypothesis. A more sensitive test of the rank-order hypothesis is to reclassify the post probability raster into nine classes using natural breaks and calculate the deposit density for the area of each of these classes using the training data. In case the deposit

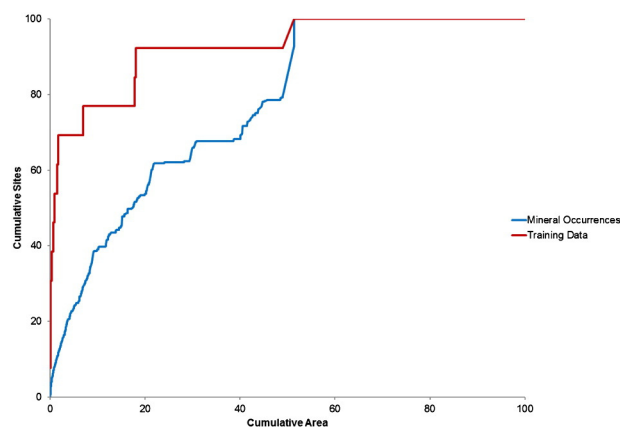


**Fig. 5.** Success rate and efficiency of prediction curves statistically test the predictive capacity of the Weights of evidence (WofE)-derived prospectivity model. The success rate curve shows training data plotted cumulatively from high to low posterior probability against the cumulative area accumulated from high to low model posterior probability. The efficiency of prediction curve shows the same except for porphyry Cu–Au occurrences replacing the training data. The sum of the area under the curves measures model performance as a percentage. The curve for the training data gave a success rate value of 99.9% whilst the curve for the mineral occurrence data gave an efficiency of prediction value of 87.6%, both confirming that the model has a high predictive efficiency that is statistically valid.



density cannot be calculated for a particular class due to a lack of deposits within the area of this class, the area can be merged with the adjacent higher posterior probability class. Results of this calculation show that deposit density increases with each increasing posterior probability class, supporting the rank-order hypothesis. The tests described above show that conditional dependence is an issue in the prospectivity model, but that analysis of the posterior probabilities by relative rather than absolute rankings is valid.

## 7. Historic exploration data

### 7.1. Database

Records of historic exploration activities and expenditure used in this study and presented in Appendix 2 (referred to here as the GEMOC database) were compiled in 2003 as part of an industry-collaborative project at the ARC National Key Centre for GEMOC, Macquarie University.

The GEMOC database was compiled from all open-file exploration reports lodged with the New South Wales government during the period 1980 to 2002 meeting the following criteria:

- The exploration licence to which the report refers had to be located within the Narromine, Dubbo, Forbes, Bathurst, Cootamundra, or Goulburn 1:250,000 map sheets (Fig. 1);
- The exploration licence to which the report refers had to cover part of the Ordovician to Silurian Macquarie Arc; and
- The focus of the reported activities had to be exploration for porphyry Cu–Au deposits.

In New South Wales, an exploration report is kept confidential for as long as the exploration licence to which the report refers is current. It is only after expiry or relinquishment of the underlying licence that the report becomes open-file and accessible to the public via an online report viewer ([www.resources.nsw.gov.au/geological/online-services/digs](http://www.resources.nsw.gov.au/geological/online-services/digs)). As such, the GEMOC database contains no records of historic exploration activities and expenditure for licences that were current in 2003.

Recorded data included: (i) Licence name and number, (ii) start and end dates, (iii) targeted mineral deposit types, (iv) work undertaken, (v) exploration stage achieved, (vi) expenditure, (vii) number of holes and metres drilled, and (viii) corporate activity (e.g., mergers, takeovers, divestures or joint ventures). For comparability all expenditure data were converted to Australian dollars at 2003 values.

The GEMOC database was used in this past study to analyse what types of exploration activities took place in the Macquarie Arc following the discovery of the Endeavour 22 porphyry Cu–Au deposit by Geopeko in 1976 and subsequent exploration boom. The data were also used to

build a basic picture of exploration success rates and industry performance for the period 1980 to 2002.

### 7.2. Main findings of the database analysis

#### 7.2.1. Principal activities

On the whole, the 346 exploration licences captured in the GEMOC database were held for 1020 years (i.e., an average of 3 years per licence) with 1400 exploration reports lodged for these licences between 1980 and 2002. Of the 1020 years of exploration, most time (61% or c. 622 years) was spent on reconnaissance activities (exploration stage B: Table 4) whilst no work was recorded for almost a fifth of this time (19% or c. 194 years). In other words, 40% of the licences recorded at least one year when no work was undertaken within these areas (Appendix 2).

The most popular types of work carried out on exploration licences within the study area were data compilation (undertaken for 87% of the licences), geological research (73%), reconnaissance geochemical sampling (73%), follow-up geochemical sampling (54%), and geological mapping (48%). Drill testing of exploration targets (exploration stage C), or resource delineation drilling (exploration stage D), were undertaken on just over a third (36%) of the licences. As illustrated by these data, licence holders preferred to embark on data compilation and reconnaissance activities rather than drilling.

#### 7.2.2. Repeat exploration

Repetition of previously undertaken exploration activities (referred to here as repeat exploration) was common within the study area. One reason for repeat exploration was that 45% of the licences changed hands more than once, whilst 19% changed hands more than twice. The maximum number a licence changed hands was six times. These ownership changes occurred either because a licence was picked up by a new party after relinquishment by the previous holder or due to corporate activities, including takeovers, mergers, joint ventures, farm-outs or sales. Other possible reasons for repeat exploration were: (i) New information or concepts, (ii) new technology, (iii) a discovery or mine development nearby, (iv) distrust, or poor quality, of previous work, or (v) corporate memory loss.

The best example for excessive repeat exploration is that of repeat reconnaissance geochemical sampling, which was undertaken more than once on 77%, more than twice on 55%, and more than five times on 14% of the licences in the study area.

#### 7.2.3. Drilling

The total number of holes drilled within the study area during the period 1980 to 2002 was 12,800. Of these holes, 10,122 (79%) were rotary air blast (RAB) holes with a combined down-hole depth of

**Table 4**

Definition of exploration stages (modified from Lord et al., 2001).

Stage	Objective	Milestones	Risks associated with successful stage progression
A	Project generation	Select and acquire ground in well endowed belts Establish data base and management system Build an expert team for the belt	Probability that this process will result in the acquisition of high quality, well-endowed and available ground that is worthy of further work
B	Prospect definition ("reconnaissance")	Build area knowledge Test presence of mineralizing system Define prospect risks Define drillable targets	Probability that this process will define drillable targets that meet criteria of the geologic model and knowledge of the area
C	Systematic drill testing	Establish size and grade potential Test potential of mineralizing system Test geologic information Test geologic and mineralization models	Probability that this process will result in one or more drill intersections of potentially economic mineralisation that warrant further drill testing
D	Resource delineation ("drill out")	Test continuity Establish controls on grade distribution	Probability that this process will result in the definition of a preliminary resource that is sufficiently robust at present prices to warrant proceeding to feasibility
E	Feasibility	Establish economic/metallurgical parameters Determine net present value (NPV) Determine project costs	Probability that the feasibility study will deliver an ore reserve

approximately 237 km. RAB drilling is typically an early-stage exploration tool commonly used to obtain bedrock samples in areas of deep weathering or cover and, thus, falls into the exploration stage B category (Table 4). According to the GEMOC database, RAB drilling was undertaken on 96 (28%) of the 346 exploration licences, presumably mainly within those where prospective bedrock is partially or almost completely under cover. Proportions of outcrop and cover were reported for 176 (51%) licences. Whilst the reported extent of cover was greater 50% in 27 (15%) and almost 100% in 117 (67%) of these licences, only 50 (28%) of these licences recorded any RAB drilling. That is even though the initial porphyry Cu–Au discovery (Endeavour 22) was made by RAB drilling in semi-covered terrain.

Reverse circulation (RC) holes ( $n = 2340$  for c. 149 km) amounted to 18% whilst diamond drill (DD) holes ( $n = 338$  for c. 31 km) accounted for only 3% of the total. RC and DD drilling are typically carried out to test a specific target or resource extensions (exploration stage C), or for the purpose of resource definition (exploration stage D).

Of the licences within the study area, 44% recorded RAB, RC and/or DD drilling. Approximately 76% of these licences recorded the first drill activity within year one or year two of the life of the licence, whilst 16% were not drilled before year three. The most extreme case was a single licence that recorded no drilling until year eight. Considering only exploration stage C- and D-type work, RC and DD drilling was undertaken on 36% of the licences. Of these licences, 62% recorded their first drilling activity within the first two years of the life of the licence.

#### 7.2.4. Expenditure

In the examined period from 1980 to 2002, a total of approximately \$68 million was spent on the 346 exploration licences covering the study area. As illustrated by Table 5, only approximately half (52%) of the total was spent on field activities with drilling accounting for a mere 22% of the total expenditure. On average, the proportion of annual expenditure committed to drilling was 19%, a figure that remained relatively constant over the examined period despite an overall increase of the number of exploration licences in the study area.

Another way of looking at the relationship between drilling and expenditure is to group expenditure by exploration stage (Table 6). As illustrated by Table 6, total expenditure recorded against the exploration stages that involve drill testing and/or resource delineation drilling (i.e., stages C, D and E) was approximately \$42 million. Given that approximately \$15 million were spent on drilling in total, the proportion of drilling expenditure in the typically drill-intensive exploration stages C, D and E was only 36%.

#### 7.2.5. Exploration stage transition and success rates

Most licences started out at exploration stage B but not all licences kept progressing from their initial exploration stage to the next (Fig. 6). In fact, most licences (i.e., 262 of 346, or 76%) within the

**Table 6**  
Expenditure by exploration stage.

Exploration stage <sup>a</sup>		Expenditure	
		2003 Dollars	Percentage
A	Project generation	\$ 1,187,661	2%
B	Prospect definition	\$ 24,721,859	36%
C	Systematic drill testing	\$ 21,453,102	31%
D	Resource delineation	\$ 16,428,503	24%
E	Feasibility	\$ 4,497,984	7%
Total		\$ 68,289,110	100%

<sup>a</sup> Letters refer to exploration stages as defined by Lord et al. (2001).

study area never progressed from their initial stage, and in most cases this stage was stage B. In other words, prospects had been defined by the holders of most licence areas but it seems that these prospects never presented valid targets for systematic drill testing, either by RC or DD.

On average, an exploration licence was held for 3 years and received expenditure commitment of \$197,000. However, none of the 346 exploration licences captured in the GEMOC database resulted in the discovery of a potentially economic mineral deposit. It is important to remember, though, that the GEMOC database is biased towards the “unsuccessful licences” because exploration reports that referred to then current licences, including those that recorded porphyry Cu–Au discoveries, were confidential. This issue was addressed by compiling information for relevant current licences ( $n = 31$ ) from company annual reports. Where no information for a current licence could be obtained, it was assigned to stage B.

Considering the “unsuccessful licences” only, (i) 63% progressed to stage B, (ii) 32% to stage C, (iii) 4% to stage D, and (iv) 1% to stage E. As illustrated in the probability graph in Fig. 7a and using the same input, the probability of a licence to progress from stage (i) A to B is 0.99, (ii) B to C is 0.36, (iii) C to D is 0.13, and (iv) D to E is 0.13. As evident in this graph, the stage transitions with the least probability of success are those from stage C to D (linked to the risk that drill testing will fail to intersect potentially economic mineralisation) and from stage D to E (linked to the risk that grade and/or tonnage of a preliminary resource are inadequate for proceeding to feasibility). The relatively low probability of advancing from stage B to C is a clear function of most licences within the study area having commenced and ended in stage B, and a general reluctance of explorers to drill.

Considering both unsuccessful and successful licences, the outcome changes significantly: (i) 59% progressed to stage B, (ii) 30% to stage C, (iii) 4% to stage D, (iv) 1% to stage E, and (v) 5% to stage F. As illustrated in Fig. 7a, the probability of a licence to progress from stage (i) A to B is 0.99, (ii) B to C is 0.41, (iii) C to D is 0.25, (iv) D to E is 0.56, and (v) E to F is 0.91. As above, the stage transition with the least probability of success is that from stage C to D, linked to the risk of failure to intersect potentially economic mineralisation. However, once a licence has reached stage D, the chances of progressing to the mining stage increase progressively. According to the cumulative probability graph shown in Fig. 7b and based on the numbers above, there was a 5% chance (odds = 1 in 20; probability = 0.05) during the period 1980 to 2002 that a licence within the GEMOC study area would progress from exploration stage A to the mining stage. This number is much higher than the typical industry success rates, which range from 1 in 24 to 1 in 100 in brownfields and 1 in 1000 to 1 in 3333 in greenfields environments (Kreuzer and Etheridge, 2010). The highly successful nature of exploration within the GEMOC study area is mainly attributable to (i) this part of the Macquarie Arc being exceptionally well-endowed, (ii) the initial recognition of the porphyry Cu–Au potential of the Macquarie Arc (i.e., 1976 discovery of the Endeavour 22 alkalic porphyry Cu–Au deposit by Geopeko Limited), and (iii) discovery of economic porphyry and skarn deposits within 20 licences that subsequently progressed to the mining stage.

**Table 5**  
Expenditure by category.

Category		Expenditure	
		2003 Dollars	Percentage
Field activities	Drilling <sup>a</sup>	\$15,049,218	22%
	Other <sup>b</sup>	\$20,540,832	30%
Salaries and on-costs		\$21,128,555	31%
Overheads		\$10,263,350	15%
Unknown		\$1,307,154	2%
Total		\$68,289,110	100%

<sup>a</sup> Includes all drilling and assaying costs.

<sup>b</sup> Includes all on-ground exploration costs (e.g., tenement costs, geochemical and geo-physical surveys, assaying, car and equipment hire, equipment operation and maintenance, travel, communication, freight).

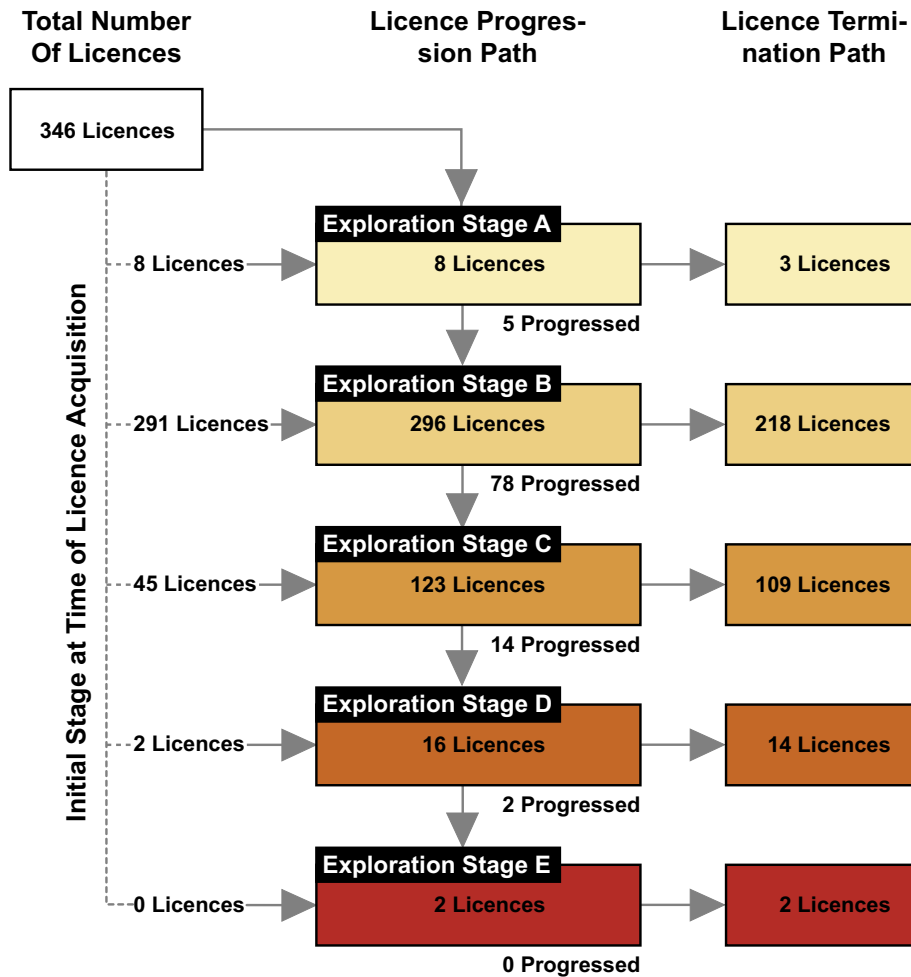


**Fig. 6.** Exploration licence progression through exploration stages as defined by Lord et al. (2001) and summarised in Table 4. The figure clearly illustrates that most of the 346 exploration licences reviewed in this study never progressed from their initial exploration stage (i.e.,  $n = 262$  or 76%), and in most cases this initial stage was stage B (reconnaissance) ( $n = 218$  or 63%). The main questions arising from this observation are: (i) Why did so many licences never progress from stage B? Or, in other words, why did they never yield any drill-worthy targets? (ii) Why did the licence holders spend so much time (on average = 2 years per licence; in total = 453 years) and money (on average = \$57,000 per licence; in total > \$12 million) on licences that never yielded any meaningful results?

## 8. Comparison of exploration expenditure and prospectivity maps

### 8.1. Creation of a combined exploration expenditure and prospectivity map

To enable the comparison of the 1980 to 2002 exploration expenditure data compiled in the GEMOC study (Fig. 1; Appendix 2) and the WofE-based prospectivity model (Fig. 4), the expenditure data had to be converted into a raster map. This translation entailed a series of key steps, including:

- Creation of a GIS polygon map: This map combines the outlines of the relevant historic exploration licences and a database attributed with licence details, most importantly the open-file exploration expenditures covering the period 1980 to 2002 (Fig. 8a). Ideally each expenditure item should have been assigned to the portion of the licence that received the exploration spent, but the GEMOC database did not lend itself to such an approach. Hence, the expenditure data were assumed to be spread uniformly across each tenement.
- Summation of expenditure in areas where licences overlap: As illustrated by Fig. 8b, the outlines of the 1980 to 2002 exploration licences overlap in space because over time certain areas were acquired more than once. Given the assumption that expenditures are spread uniformly across each licence, areas of licence overlap represent areas of combined expenditures. The expenditure for each overlapping licence partition was calculated as a proportion of the area of the licence

partition to the total area of the licence. The total expenditure for each overlapping licence partition was then summed using the GIS.

- This step allowed the map to be coloured by total expenditure for all overlapping licence areas, which highlights the areas that received the greatest exploration expenditure (Fig. 8c).
- Fitting of the post probability map: The next step was to clip the WofE-based post probability map (Fig. 8d) to the area defined by the exploration licences captured in the GEMOC study. Subsequently, the post probability map was further refined to only include those licences for which historic expenditure data were available (Fig. 8e).
- Conversion to a raster map: The total expenditure map (Fig. 8c), which is a collection of polygons, had to be converted to a raster map to facilitate comparison of the total expenditure map and the post probability map, which is a raster grid. A unique conditions raster of all the possible unique post probability and total expenditure values was created to simplify the analysis. This allowed the mapping of the post probability values to the of the licence partition areas (Fig. 8e).
- Calculation of an expenditure efficiency attribute: This attribute, which was calculated by multiplying the post probability values by the total licence expenditure, was used to map the areas characterised by high geological potential and high exploration expenditures (Fig. 8f). Areas of low geological potential are basically eliminated in this operation because of their low post probability values (<0.000131), facilitating the recognition and mapping of those areas where exploration expenditure was efficiently allocated.

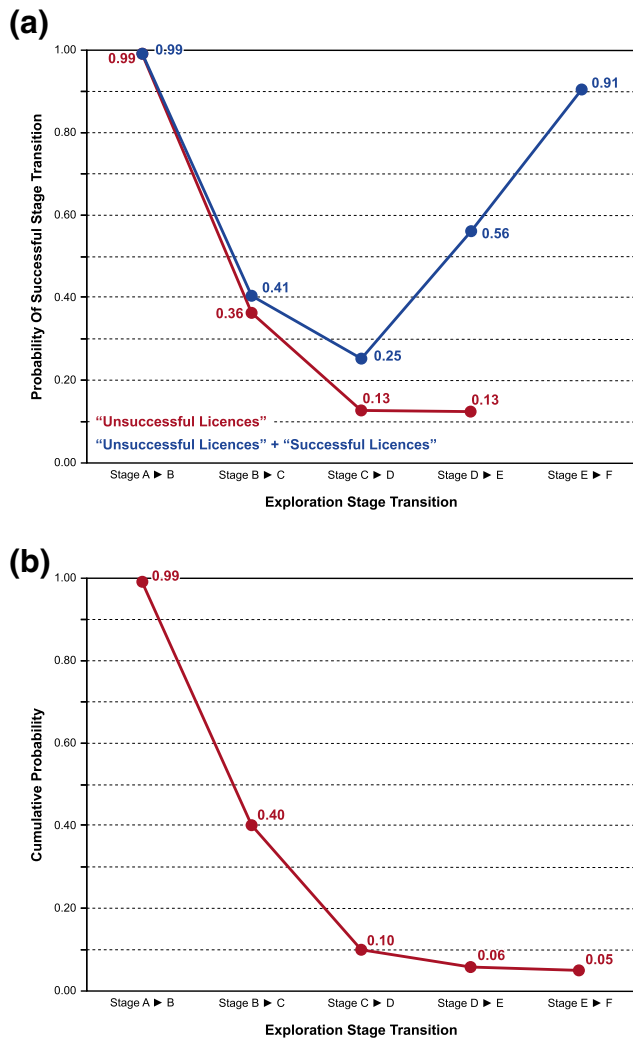


**Fig. 7.** Probability profiles for the GEMOC study area. (a) Probability of a licence progressing from one stage of exploration to the next. The red line represents the "unsuccessful" licences only whereas the blue line represents both the "unsuccessful" and "successful" licences (see text for details). As evident in this graph, the stage transitions with the least probability of success are those from stage C to D (linked to the risk that drill testing will fail to intersect potentially economic mineralisation) and from stage D to E (linked to the risk that grade and/or tonnage of a preliminary resource are inadequate for proceeding to feasibility). The relatively low probability of advancing from stage B to C is a clear function of most licences within the study area having commenced and ended in stage B, and a general reluctance of explorers to drill. (b) Cumulative probability graph illustrating that during the period 1980 to 2002 there was a 5% chance that a licence would progress through all stages of exploration and yield a mining operation. This number is relatively high compared to typical industry success rates (Kreuzer and Etheridge, 2010) indicating that exploration within the GEMOC study area was highly successful.

## 8.2. Spatial analysis of porphyry Cu–Au exploration expenditure

### 8.2.1. Expenditure as a function of exploration stage and area

Mineral exploration programs are commonly staged (Lord et al., 2001) with each stage designed to get to the next decision point, that is, whether or not to continue exploring a particular area based on results of the previous exploration stage. As a general rule, each consecutive exploration stage is more expensive due to the progressively more detailed nature of the work required (Roscoe, 2002). Table 7 provides a summary of typical exploration cost requirements per exploration stage in the Macquarie Arc based on the data compiled in the GEMOC study.

The licence expenditure map (Fig. 8c) was classified according to potential stage of exploration based on the total expenditure attribute using the cost ranges in Table 7. The total area covered by

exploration licences active between 1980 and 2002 and with open-file expenditure information was 34,793 km<sup>2</sup> (Table 8). Approximately 42% (14,630 km<sup>2</sup>) of this area received total expenditures less than \$39,000, which equates to the initial data review for licence acquisition. About 11,610 km<sup>2</sup> (c. 33%) received the minimum expenditure to allow targeting to have been carried out on the licence, whilst 4349 km<sup>2</sup> (c. 12%) received sufficient expenditure for geological, geochemical and geophysical data acquisition to test the initial target areas on the licences. Only 4204 km<sup>2</sup> (c. 12%) of the total area received sufficient expenditure to allow for some level of drilling to be carried out. Importantly, more than 75% of the total licence area did not receive enough expenditure to allow for any type of drilling during the tenure of the licence, which is the most important tool for collecting subsurface information, testing geological concepts and locating and defining potentially economic mineralisation.

In the period 1980 to 2002, approximately 18,000 km<sup>2</sup> (c. 56%) of the total licence area were held under one licence only, whereas only about 1400 km<sup>2</sup> (4%) were held under more than four licences. Between 1980 and 2002, a total of approximately \$70 million was spent on exploration activities within the overall licence area. Interestingly, this total can be divided into two roughly halves with approximately 51% (just over \$35 million) spent on early-stage activities such as ground acquisition and target definition and testing (i.e., exploration stages A and B) and c. 49% (just under \$35 million) spent on drill testing and feasibility studies associated with the more advanced exploration stages C to E. This result ratifies a similar finding described in Section 7 and further corroborates the notion of a widespread preoccupation by explorers with early stage work and a general reluctance to drill, both of which resulted in most licences starting and ending in exploration stage B (Fig. 6).

The tendency for area reduction, a typical function of the narrowing of focus to progressively smaller areas as licences progress from one stage of exploration to the next, is illustrated well by the distribution of exploration expenditures with the 13% of the total licence area that had reached exploration stages C, D or E, having received almost half (c. 49%) of the of the total expenditure (Table 8).

### 8.2.2. Exploration effectiveness

The main aim of any analysis of historic exploration is to assess how effective exploration was in relation to known geological potential and in the context of data availability, geological understanding, corporate strategies and business models and government policy. Assuming that historic exploration in the GEMOC study area was effective, the highest exploration expenditure should have occurred in the areas of greatest geological potential (i.e., highest post probability values).

There are various ways of testing this relationship and the basic statistical information for the combined licence expenditure and geological potential data are summarised in Table 8. About 23,000 km<sup>2</sup> of the combined licence area have low geological potential, which equates to approximately 72% of the GEMOC study area. In comparison, about 24,000 km<sup>2</sup> of the licence area received low exploration expenditures (\$130,000 or less), which also equates to approximately 75% of the total area. If exploration investment was efficiently targeted one would expect that both variables received equal proportions of the total exploration expenditure. However, the spatial analysis reveals that total of \$23 million (c. 33%) were spent on licences that recorded low exploration expenditure whereas approximately \$44 million (c. 62%) were spent on licences covering areas of low geological potential. That is almost double the total investment recorded by the licences with low exploration expenditure. Based on these data it is likely that a significant amount of expenditure was misdirected into areas of low geological potential. Conversely, less than \$10 million (c. 14%) were invested in areas of high geological potential.

Another way of comparing the relationship between exploration spent and geological potential is to plot both variables in a scatter plot to test their spatial statistical relationship (Fig. 9). In a scenario where

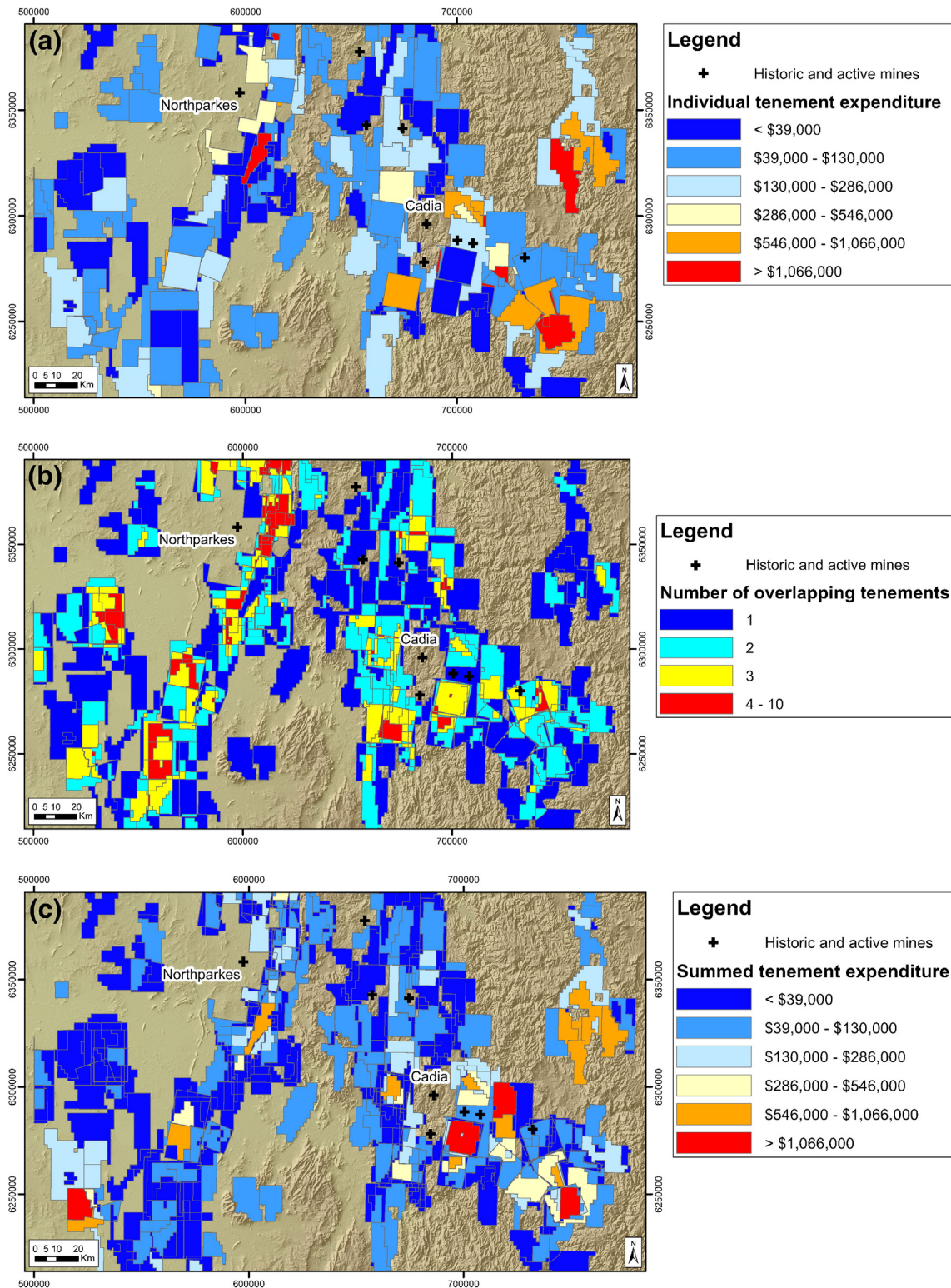


**Fig. 8.** Licence expenditure maps covering the greater Cadia and Northparkes districts. (a) Unprocessed licence expenditure map. Given that ArcGIS draws map symbols in a specific order (i.e., symbol level drawing), only tenement polygons that “sit on top” are visible in full. Underlying polygons, on the other hand, are either partially or completely obscured. To make the spreadsheet based input data amenable to spatial modelling, the assumption was necessary that expenditure was uniformly spread across each licence. Digital licence vector data (i.e., tenement polygons) were sourced from: [www.resourcesandenergy.nsw.gov.au/miners-and-explorers/geoscience-information/online-services/minview](http://www.resourcesandenergy.nsw.gov.au/miners-and-explorers/geoscience-information/online-services/minview). (b) Partitioned licence expenditure map accounting for licence overlap. (c) Summed licence expenditure map adding exploration expenditures in areas where licences overlap. (d) Post probability map of porphyry Cu–Au potential. (e) Post probability map of porphyry Cu–Au potential clipped to exploration licence areas with recorded expenditure. (f) Combined post probability and licence expenditure map illustrating areas where high expenditure and high geological potential match. These areas (represented by red and yellow colours) have been effectively explored, whereas the remaining area (represented by light and dark blue colours) has not. (g) Post probability values of porphyry Cu–Au potential superimposed on summed licence expenditure map illustrating the general discrepancy between areas of high expenditure and areas of greatest geological potential. This discrepancy is taken to imply the inefficient nature of past exploration expenditure outside the main mining areas.

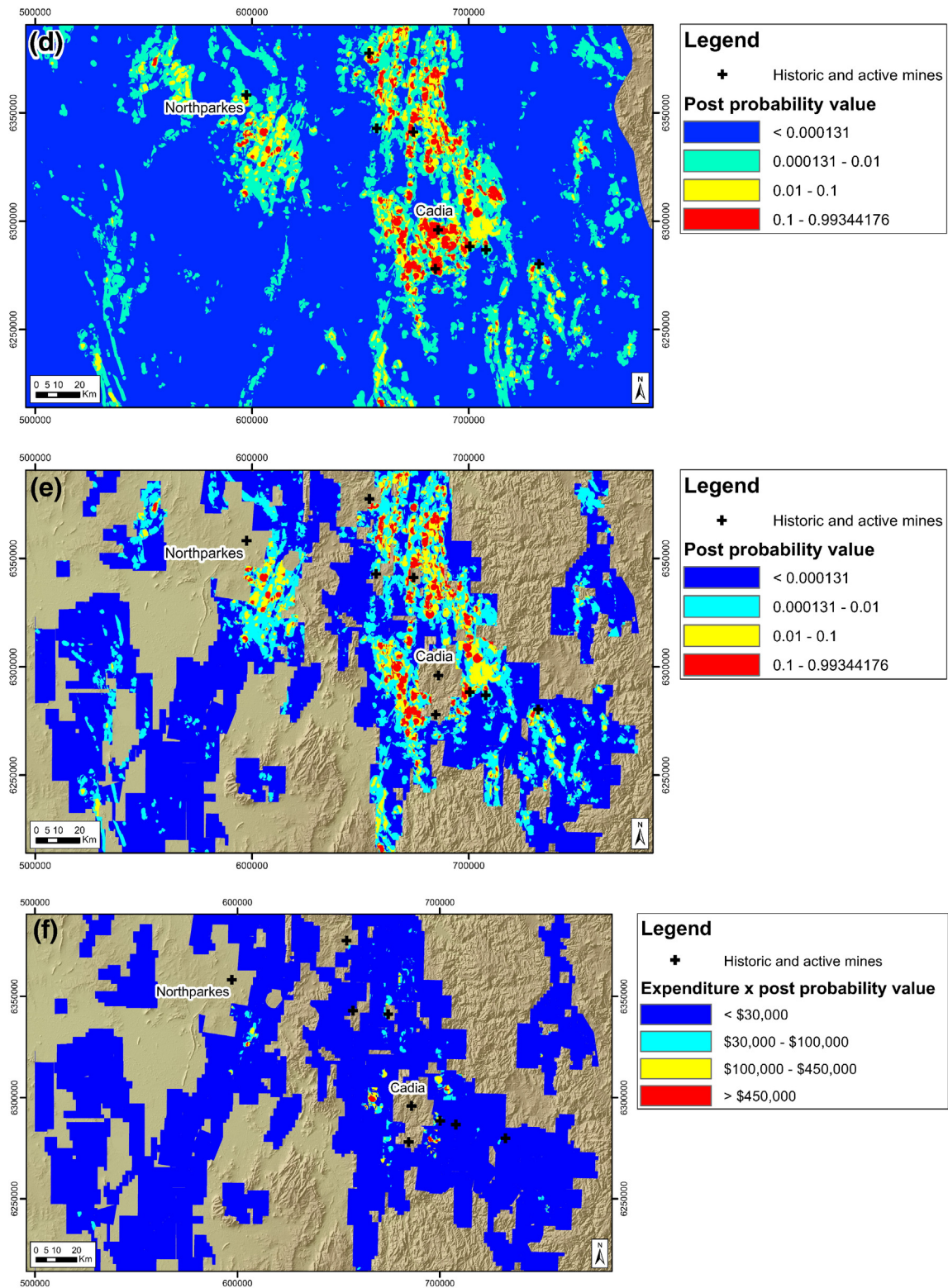


Fig. 8 (continued).

exploration investment is being effectively directed into areas of higher geological potential (i.e., equal to or higher than post probability values of 0.01), one would expect the scatter plot to display a statistically valid positive correlation with a regression line from low expenditure values and low post probability values at  $45^\circ$  to high expenditure values and high post probability values. In the actual dataset, the correlation between post probability values and exploration expenditure is low

( $R^2 = 0.14$ ), indicating that there is only a weak correlation between exploration expenditure and geological potential. This correlation is biased to some extent by the unavailability of expenditure data for the historic and operating mine areas that would plot in the upper right of the graph (high post probability values, high exploration expenditures). Their inclusion would improve the correlation result. The scatter plot in Fig. 8 is subdivided into four domains relating to the classifications

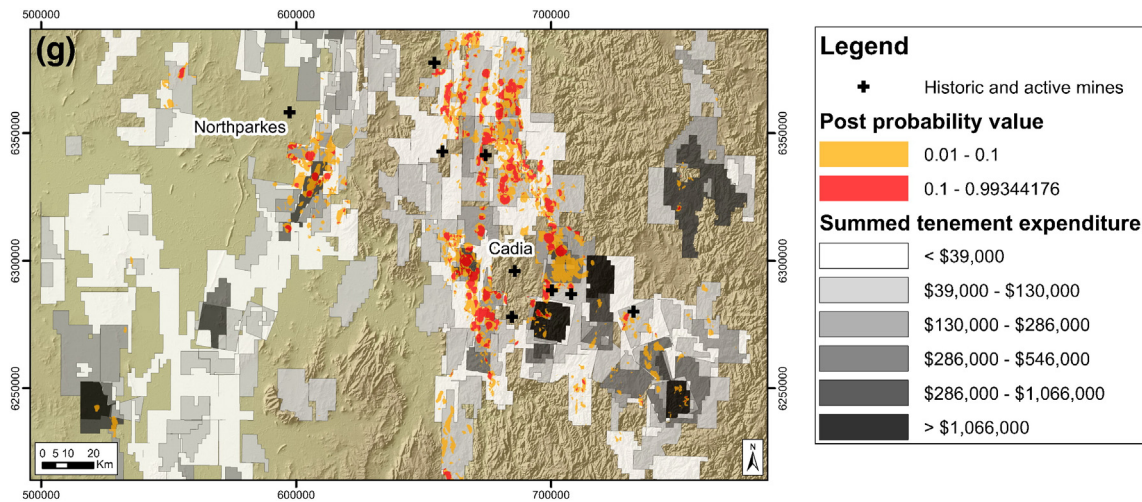


Fig. 8 (continued).

used for exploration expenditure and post probability values in Tables 7 and 9. As illustrated in Fig. 8, a large proportion of the geologically prospective area covered by the licences has received insufficient expenditure for adequate testing of geological targets, in particular drilling. This is confirmed by the 603 km<sup>2</sup> area classified as low expenditure, high probability target (Table 8), which is a surprisingly large area of prospective ground for a region that has recorded significant historical porphyry Cu–Au exploration and development and is commonly considered a mature exploration destination.

The post probability values range from close to zero in areas of the lowest geological potential to one in the areas of high geological potential. Consequently areas of effective exploration expenditure can be mapped by multiplying the total expenditure by the post probability values. Any expenditure in non-prospective areas will be reduced close to zero allowing areas of effective exploration to be mapped (Fig. 8f). There are 692 km<sup>2</sup> of highly prospective ground covered by the licences investigated in this study, but only 89 km<sup>2</sup> or 12.9% of the prospective ground has been explored effectively (i.e., has had some form of drilling). The remainder, which totals 603 km<sup>2</sup>, has not yet been effectively tested. If, for the area above, the prior probability is considered worthy of exploration investment, especially for areas with missing data, then the untested area increases significantly. Overall, the results of our analysis indicate that

although exploration and mining have been carried out for more than 100 years in the study area much of the prospective area remains untested and should be of interest for further exploration investment (Fig. 8g).

## 9. Discussion

### 9.1. Prospectivity model

The post probability values for the area clipped to the GEMOC tenement areas range from 0.00000002 over the non-prospective areas through to 0.99344176 over the most prospective areas. The highest post probability values have similar values to the known mines at Cadia Valley (0.993442), Yeoval (0.966633), Browns Creek (0.975332) and Northparkes (0.154682). The post probability values for the prospective areas in the tenement study area do not include the mine areas as there are no publically available expenditure data for these areas. However, there are areas in the tenement study area with similar post probability values to the mine areas meaning they have similar geological, geochemical and geophysical attributes to the known mines in the district. Areas were defined as unprospective if they had post probability values less than the prior probability for the regional model of 0.000131 (i.e., the chance of randomly finding a deposit in

Table 7

Average costs (in 2003 dollars) associated with a staged exploration program in the Macquarie Arc, 1980 to 2002.

Exploration stage <sup>a</sup>	Typical work program/aims	Exploration cost <sup>b</sup>	Administration cost <sup>c</sup>	Total cost	Cumulative cost
A Ground acquisition	Historic data compilation and review; identification of the most prospective ground available	\$30,000	\$9,000	\$39,000	\$39,000
B Target definition	Detailed historic data compilation, generation of empirical and/or conceptual target areas; reconnaissance exploration of target areas (e.g., historic mines or prospects, untested anomalies, conceptual plays)	\$70,000	\$21,000	\$91,000	\$130,000
Target testing	Acquisition of geochemical, geophysical and more detailed geological data to define drill targets	\$120,000	\$36,000	\$156,000	\$286,000
C Drill testing	Drill testing of targets; assessment of grade and continuity of any mineralisation discovered; acquisition of 3D geological data; testing of geological concepts	\$200,000	\$60,000	\$260,000	\$546,000
D Resource delineation	Drill testing of any potentially economic mineralisation discovered to better define size, grade and continuity of the orebody	\$400,000	\$120,000	\$520,000	\$1,066,000
E Feasibility	Feasibility studies into developing a profitable mining operation	\$12,000,000	\$3,600,000	\$15,600,000	\$16,666,000

<sup>a</sup> Letters refer to exploration stages as defined by Lord et al. (2001).

<sup>b</sup> Cost estimates are based on the data compiled in the GEMOC study. The costs associated with exploration stage E can vary between tens and hundreds of millions of dollars depending on the size of the potential operation. For example, based on data extracted from Newcrest Mining Limited's annual reports and the company's reported average discovery costs per ounce of gold, the Cadia mine (part of Newcrest's Cadia Valley operation within the GEMOC study area) incurred an estimated total exploration expenditure in the range from \$120 to \$265 million and development costs of at least \$400 million. Expenditures on projects that were successful were not recorded in the GEMOC study due to the confidential nature of reports that referred to then current licences.

<sup>c</sup> An administration and management cost of 30% has been assumed for each stage of exploration.

**Table 8**  
Expenditure and coverage statistics for the tenement, prospectivity and combined tenement and prospectivity maps in the Lachlan Fold Belt.

Class	Area category	Tenement area		Geological potential		Combined		Combined expenditure	
		Area km <sup>2</sup>	Percentage	Area (km <sup>2</sup> )	Percentage	Area (km <sup>2</sup> )	Percentage	2003 dollars	Percentage
Expenditure	Total area	34,793	100.0%	101,555	100%	32,265	100.0%	\$69,942,999	100%
	Licence areas with expenditure < \$39 K (Stage A)	14,630	42.1%	–	–	13,116	40.7%	\$ 9,286,197	13.3%
	Licence areas with expenditure \$39 K to \$130 K (Stage A)	11,610	33.4%	–	–	10,906	33.8%	\$13,798,465	19.7%
	Licence areas with expenditure \$130 K to \$286 K (Stage B)	4349	12.5%	–	–	4038	12.5%	\$12,364,072	17.7%
	Licence areas with expenditure \$286 K to \$546 K (Stage C)	1784	5.1%	–	–	1784	5.5%	\$10,026,519	14.3%
Overlap	Licence areas with expenditure \$546 K to \$1066 K (Stage D)	1462	4.2%	–	–	1462	4.5%	\$10,634,706	15.2%
	Licence areas with expenditure > \$1066 K (Stage E)	958	2.7%	–	–	958	3.0%	\$13,833,040	19.8%
	Areas with no licence overlap	19,731	56.7%	–	–	18,212	56.4%	–	–
	Areas with 2 to 4 licence overlaps	13,593	39.1%	–	–	12,642	39.2%	–	–
	Areas with >4 licence overlaps	1469	4.2%	–	–	1412	4.4%	–	–
Prospectivity	Unprospective areas (<0.000131)	–	–	85,584	84.3%	23,354	72.40%	\$43,598,402	62.3%
	Moderately prospective areas (0.000131 to 0.01)	–	–	12,422	12.2%	6497	20.10%	\$16,870,891	24.1%
	Prospective areas (0.01 to 0.1)	–	–	2440	2.4%	1722	5.30%	\$5,432,763	7.8%
	Highly prospective areas (>0.1)	–	–	1109	1.1%	692	2.10%	\$4,040,943	5.8%
	Highly prospective areas with low expenditure	–	–	–	–	603	2.70%	–	–
	Highly prospective areas with high expenditure	–	–	–	–	89	0.30%	–	–

the area). Any values greater than the prior probability were defined as having some geological potential and these cover only approximately 16% of the study area, resulting in a significant reduction of the search area. The areas with the most significant geological potential are defined as any cell with a post probability value greater than 0.1 as this includes the majority of the known historic and operating mines in the area, which reduces the search area to around 2% of the tenement area or 690 km<sup>2</sup> compared to a total search area of 32,265 km<sup>2</sup>. There are 2177 separate targets within this area that have similar geology, geochemistry and geophysical attributes as the areas covered by the main historic and operating mines. These targets have been attributed with the maximum post probability value for each area which allows the target areas to be sorted and prioritised according to geological potential. A total of 79 of these target areas have historic copper or gold occurrences within their areas. The remaining target areas are new exploration opportunities for future investment. It is also possible to evaluate whether these targets have been effectively tested by historic exploration by incorporating the GEMOC exploration expenditure data as an attribute for each target area.

As discussed above, conditional dependence is an issue with the post probability values that may introduce bias into the model. One way to resolve issues with conditional dependence is to combine or exclude

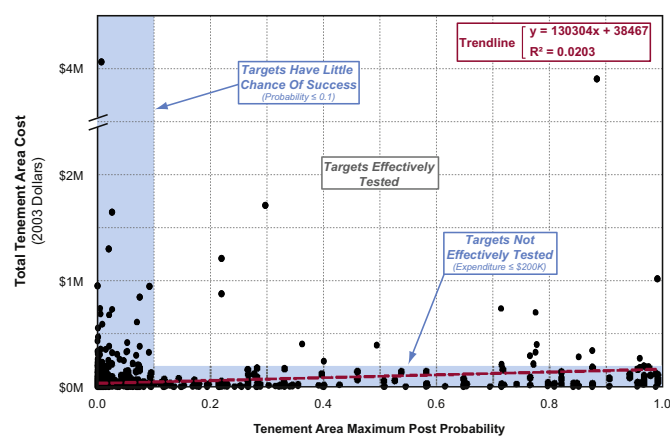


**Fig. 9.** Scatter plot of post probability (i.e., geological potential) versus expenditure data for the exploration licences examined in this study. The trend line indicates a weak positive correlation ( $R^2 = 0.02$ ) between post probability and exploration expenditure values.

predictor maps. Whilst statistically valid, such an approach will result in information being lost when results are analysed and exploration targeting is done. The identification of missing data is critical for exploration targeting as it may not be the targets with the highest post probability values that offer opportunities for successful discovery, but targets with high post probability values and missing data that have not been acquired to date. These targets can be easily identified using the tools in GIS and ranked and prioritised accordingly. This type of targeting is particularly useful for exploration as the type of missing data that could add to the prospectivity of a target if present helps constrain future exploration planning and budgeting objectively.

## 9.2. Historic exploration

When wide-spaced reconnaissance drilling by Geopeko Limited in 1976 intersected the Endeavour 22 Au-rich alkalic porphyry deposit (Lye et al., 2006), it triggered a significant increase of exploration activity within the Macquarie Arc targeting this previously unrecognised style of mineralisation. Within 20 years of the initial discovery, the Macquarie Arc had emerged as the largest porphyry province in Australia with a resource base of greater than 80 Moz of Au and 13 Mt of Cu (Clancy Exploration Limited, 2009; Cooke et al., 2007) supporting significant, long-life mining operations such as at Cadia and Northparkes.

Given the above, there is no doubt that, taken as a whole, exploration in the GEMOC study area was very successful. For example, during the study period of 1980 to 2002 there was a 5% chance (probability: 0.05; odds = 1 in 20) that a licence would progress through all stages of exploration and yield a mining operation (Fig. 7b). This number is much higher than typical industry success rates (Kreuzer and Etheridge, 2010), again corroborating the successful nature of exploration within the GEMOC study area. Moreover, the 5% success rate achieved by industry is 250 times greater than the 0.000216 prior probability (chance = c. 0.02%; odds = 1 in 5000) for discovery of porphyry Cu–Au deposit within the GEMOC study area. However, whilst exploration as a whole was highly successful, this success was only shared by a select few companies.

The GEMOC database, which is biased towards the unsuccessful licences, provided some clues as to what may have gone wrong for the majority of the explorers with the reluctance to drill presenting itself as one of the most serious issues. Overall, only 44% of the licences recorded any RAB, RC or DD drilling with 24% of these licences not having seen any drill activity before year three of their tenure. A staggering 56%



**Table 9**Classified prospectivity of the study area based on the post probability values from the WofE model of the Lachlan Fold Belt<sup>a</sup>.

Prospectivity	Definition	Post probability	Area covered	Follow-up
Unprospective	Any cell with a value less than the prior probability of 0.000131; contains no, or only few, predictive map variables	<0.000131	84.30%	No action
Prospective	Cells with a value greater than the prior probability but characterised by a minimum number of predictive variables or missing data	0.000131 to 0.01	12.20%	Check areas where important input data are missing
Priority targets	Cells containing most of the required predictive map variables but with some variables missing or characterised by missing data like the North Parkes District where prospective geology is mainly under cover	0.01 to 0.1	2.40%	Check for missing data; field check for presence of predictive map variables
High priority targets	Cells with values in the range of the known mines such as North Parkes (0.154682), Yoeval (0.966633), Browns Creek (0.975332) and Cadia (0.993442)	>0.1	1.10%	Check for missing data; plan follow-up drilling or exploration data acquisition to check for presence of predictive data

<sup>a</sup> Lower cut-off = prior probability; upper cut-off = minimum post probability value for the main porphyry Cu–Au mines in the Lachlan Fold Belt.

of the licences never recorded any drilling at all. The big question here is why? Whilst market forces would have played some role in this (e.g., downturns in 1983, 1987 and 1999, the Bre-X scandal in 1997, and generally depressed gold prices between 1983 and 2002) the proportion of licences that recorded any drilling and the expenditures attributed to this drilling remained more or less constant over the almost 20 years of investigation. As such, it is unlikely that market forces alone would have controlled the observed patterns. But why did drilling rates stay constant over time when the belt became increasingly more data-rich and knowledge progressively increased? Theoretically, it should get easier and quicker to progress from exploration stage B to stage C as knowledge and data availability increase, thereby resulting in a proportional increase of drilling over time. However, none of this occurred in the study area. Potential reasons for the above include explorers not using new data effectively, poor science, lack of objectivity, market driven exploration, ground locked up by successful explorers who see prospectivity differently to new juniors entering the area for the first time, or the market not allowing companies to raise sufficient funds to drill. Whatever the reason, increased knowledge and data availability did not translate into explorers' ability to define drill-worthy targets, at least not outside the main mining areas.

Further to the above, only 28% of the licences where bedrock is partially or fully obscured by cover recorded any RAB drilling. That is despite RAB drilling providing a relatively inexpensive but highly effective geochemical sampling tool for areas under (partial) cover. It is this type of drilling that is most important in making discoveries under cover as illustrated by its crucial role in the initial discovery of alkalic porphyry Cu–Au mineralisation at Endeavour 22 in semi-covered terrain. Unfortunately, past explorers were generally reluctant to drill through the cover to see what is there and, thus, in the absence of any compelling conceptual, geochemical or geophysical targets did not commit to any drilling at all. In fact, a general bias against exploring more poorly-known areas under cover (Fig. 10) may present another explanation for the apparent inefficiency of previous exploration within the study area. When exploration decision makers evaluate an exploration project in terms of exploration risks and the probability of making an economic discovery, they often use the heuristic (mental shortcut) that areas where it is more certain that mineralisation is present (e.g., in the vicinity of exposed mineral occurrences) are lower risk when in many cases the opposite is true (J.M.A. Hronsky, pers. comm., 2014).

Overall, the above scenarios are most easily explained by heuristics and biases in judgement and exploration decision-making (cf. Wastell et al., 2011), and / or explorers being focused on other projects elsewhere, not turning over ground efficiently or hanging on to ground that is not worth keeping (i.e., “pet project syndrome”), thereby wasting time and investor dollars. A point in case is the fact that most licences (i.e., 262 of 346, or 76%) never progressed from their initial stage, and in most cases this stage was stage B. A comparison between the WofE

prospectivity model and the area covered by licences that started and ended in stage B illustrates that approximately 72% of these licences were situated on unprospective ground. This finding offers an explanation as to why so many of these licences never yielded any drill-worthy targets. But why were these licences acquired in the first place? On the flip side: Why did the remaining 28% of these licences not yield any drill-worthy targets when these licences covered prospective ground? This ground includes areas with post probabilities between 0.01 and 0.1 that contain most of the required predictive map variables (c. 5%) and even areas with high-priority targets characterised by post probabilities greater 0.1. The latter cases clearly fall into the category of opportunity wasted.

It is possible that, if the recorded exploration investment had been used to effectively test the areas of greatest geological potential, additional mines may have been discovered during the period investigated in this study. This point again reiterates how critical it is for explorers to focus the limited funds available into the most prospective areas as early in the exploration process as possible.

### 9.3. Comparison of prospectivity and historic exploration data

Cowley et al. (2009) argued that the spatial distribution and density of exploration activities may be taken as a spatial measure of prospectivity as perceived by the minerals exploration industry. Based on this premise, they produced “exploration values maps” of past and current tenements, drillhole locations, mineral occurrences, gravity stations, aeromagnetic surveys and geochemical sample locations covering the northern Finders Ranges, South Australia. According to Cowley et al. (2009), these maps showed clear alignment of sustained exploration interest and computed prospectivity. The maps also helped to identify areas of high prospectivity that have not received elevated exploration interest.

Our comparison of prospectivity and historic exploration data is based on similar principles although we used exploration expenditure as the principal measure of prospectivity as perceived by the minerals exploration industry. The main limitations to our approach were:

- The lack of detailed information regarding the spatial distribution of exploration expenditure within each licence. To make the spreadsheet based expenditure data amenable to spatial modelling, the assumption was necessary that expenditure was uniformly spread across each licence. Obviously, this is not normally the case because exploration would focus on those parts of a licence that are perceived most prospective. Any future modelling should aim to incorporate exploration datasets such as drill hole and geochemical sample locations to link expenditure to specific areas within each licence and use the total licence expenditure to account for costs that are spread across the entire licence, such as administration costs.

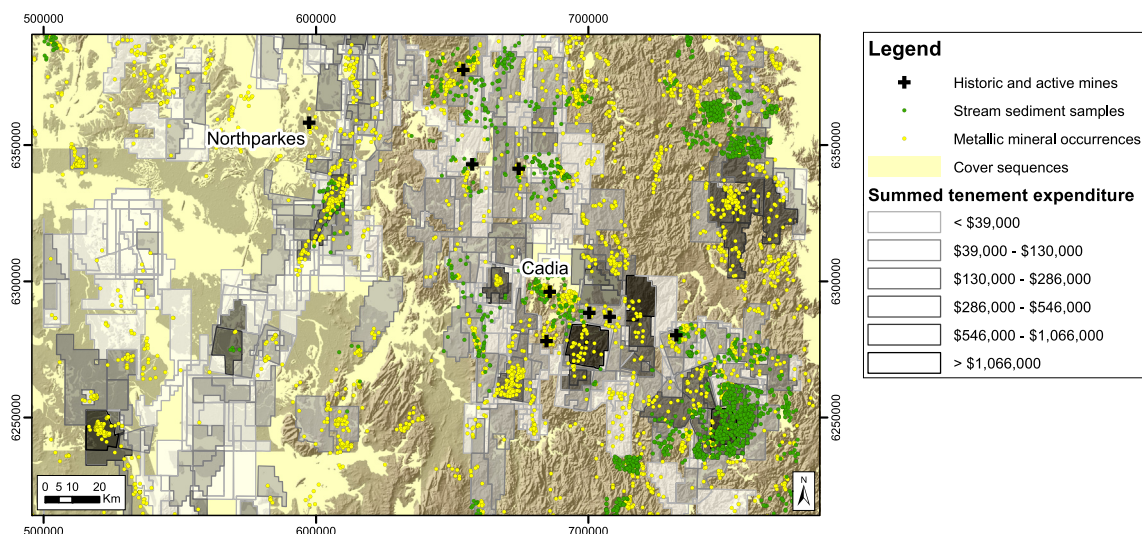


**Fig. 10.** Distribution of exploration expenditures (as shown in Fig. 8c) relative to the distribution of post-mineralisation cover, stream sediment sample locations and mineral occurrences (with the latter two serving as proxies for domains of bedrock exposure within the study area). As illustrated by this figure and as common in many exploration destinations worldwide, the tenements that received the lowest summed expenditures (i.e., < \$39,000) are mainly in areas of cover and/or areas of low mineral occurrence density (i.e., areas with a mineral occurrence density that is 2.3 orders of magnitude less than that of the \$39,000–\$130,000 summed tenement expenditure category, and 9.6 orders of magnitude less than the > \$1,066,000 category). This expenditure distribution is perhaps best explained in terms of a general bias against exploring more poorly-known areas under cover. When exploration decision makers evaluate an exploration project in terms of exploration risks and the probability of making an economic discovery, they often use the heuristic (mental shortcut) that areas where it is more certain that mineralisation is present (e.g., in the vicinity of exposed mineral occurrences) are lower risk when in many cases the opposite is true (J.M.A. Hronsky, pers. comm., 2014).

- The lack of expenditure data for active licences. These data were confidential and not available but it is important that any future study addresses this issue by either finding ways of acquiring the actual expenditure data or by calculating a proxy for exploration expenditure over these areas.
- Uncertainty about the potential impact on any expenditure analysis of: (i) Explorers initially acquiring larger than required licence areas that, because of legislative requirements for area reduction over the life of a licence, will later need to be reduced, and (ii) anecdotal evidence of explorers allocating expenditure, particularly management and administrative costs, from other licences to licences that would otherwise not meet annual minimum expenditure requirements as set by the government. To some degree, these aspects and market driven issues, like using tenement acquisition near recently discovered mines to raise funds for exploration on unrelated projects, may help explain expenditure directed towards areas of low prospectivity.

Despite these limitations, the spatial analysis of exploration expenditure comparison of the expenditure and prospectivity maps delivered outcomes not only corroborating the database analysis (e.g., that most of the exploration investment outside the main mining areas has potentially not been efficiently targeted, in that this expenditure was not directed towards the areas of highest geological potential: Figs. 7 and 8, Table 8), but also significantly augmenting the database analysis (e.g., that prospective but underexplored areas exist within the study area that represent significant targets for future acquisition and exploration, and that the government legislation to manage and maximise benefit to the state from that investment is not operating as effectively as it could to develop the states mineral resources).

#### 9.4. Implications for mineral exploration

According to a recent quantitative resource assessment by Bookstrom et al. (2014), the Macquarie Arc may contain seven as-yet-undiscovered porphyry Cu–Au deposits, all expected to occur within one kilometre of the current land surface. At the 0.5 probability level, these as-yet undiscovered deposits are estimated to contain 2900 Mt of ore, which is equal to 69% of the identified porphyry Cu–Au resources

within the Macquarie Arc based on figures presented by Bookstrom et al. (2014).

Given the above and the findings of our study suggesting that past exploration did not efficiently test the prospective area, significant potential remains for discovery in the Macquarie Arc of additional, sizeable porphyry Cu–Au deposits.

#### 9.5. Future developments

We regard this work as a stepping stone to developing an integrated methodology harnessing the power of spatial analysis and GIS-based prospectivity modelling to inform conceptual mineral deposit models and financial and geological risk and decision analysis using Monte Carlo simulation and decision trees, and vice versa. By spatially enabling mineral deposit, risk and decision models, we could develop a powerful workflow and tool for (i) testing and calibrating geological models, (ii) project / portfolio valuation and ranking, (iii) measuring the value added by exploration investments, and (iv) measuring exploration maturity. The economic benefit of a geological process-based risk analysis approach to exploration targeting has been successfully demonstrated by the petroleum industry (e.g., Rose, 1999; Suslick and Schiozer, 2004).

### 10. Summary and conclusions

- This study compared a prospectivity map that reflects porphyry Cu–Au potential to a map of exploration expenditures that serve as a spatial measure of porphyry Cu–Au potential as perceived by the minerals exploration industry.
- The study area is defined by the Narromine, Dubbo, Forbes, Bathurst, Cootamundra, and Goulburn 1:250,000 scale map sheets, and centred upon the Ordovician to Early Silurian Macquarie Arc in New South Wales, Australia's most significant porphyry province (>80 Moz Au, >13 Mt Cu).
- Exploration activity and expenditure data were compiled from all open-file exploration reports lodged between 1980 and 2002 for exploration licences targeting porphyry Cu–Au deposits. This period reflects a time of increased exploration activity within the Macquarie Arc following the initial discovery of the

Endeavour 22 (Goonumbla) Au-rich alkalic porphyry deposit by Geopeko Limited in 1976.

- (iv) A weights of evidence (WofE) model of porphyry Cu–Au prospectivity was developed in the framework of a mineral systems approach covering the entire eastern Lachlan Fold Belt in New South Wales. For the purpose of this investigation, the model was clipped to fit the study area defined above, allowing direct comparison of the prospectivity model and historic exploration data.
- (v) Taken as a whole, exploration in the study area was highly successful, resulting in a 5% chance of an exploration licence progressing through all stages of exploration to yield a mining operation. This number is much higher than typical industry success rates. However, this success was only shared by a select few companies. Most of the exploration investment outside the main mining areas has potentially been poorly targeted in that expenditure was not directed towards the areas of highest geological potential. As at 2002, many prospective areas identified in the prospectivity analysis remained un(der)explored, including some priority targets. As such, the Macquarie Arc had not yet reached exploration maturity, despite over two decades of exploration subsequent to the discovery of Endeavour 22 in 1976.
- (vi) The analysis revealed a general reluctance to drill with only 44% of exploration licences having recorded any RAB, RC or DD drilling. Of these, 24% did not record any drill activity before the third year of tenure. A staggering 56% of the licences never recorded any drilling at all.
- (vii) Equally startling is the fact that 76% of exploration licences never progressed from their initial stage, and in most cases this stage was stage B (i.e., prospect definition / reconnaissance). A comparison between the WofE prospectivity model and the area covered by licences that started and ended in stage B illustrates that approximately 72% of these licences were situated on unprospective ground. The latter finding offers a possible explanation as to why so many licences never yielded any drill-worthy targets.
- (viii) The outcomes of the spatial and statistical comparison have implications for assessing the effectiveness of exploration investment and exploration maturity, both of which are key inputs for exploration decision-making.
- (ix) The outcomes also have implications for strategic planning of future government legislation designed to manage and maximise the benefits from exploration investment.
- (x) The approach adopted in this study could be used in the future to measure the effectiveness of exploration targeting and investment, either on behalf of exploration companies wanting to evaluate current or past exploration programs or on behalf of government organisations wanting to evaluate their exploration initiatives. As such, our approach may also be used as a guide with respect to the types of data to be collated and modelled and GIS tools and work flows required to allow this type of analysis to become standard practise in the industry. This type of information will better inform governments and investors of the performance of exploration companies and provide a more objective measure of assessing exploration maturity.

Supplementary data to this article can be found online at <http://dx.doi.org/10.1016/j.oregeorev.2014.09.001>.

## Acknowledgements

This work is based on historic exploration and expenditure data compiled as part of an industry-collaborative research project at the ARC National Key Centre for Geochemical Evolution and Metallogeny of Continents (GEMOC), Macquarie University, Sydney. We acknowledge past financial support of this research project by Macquarie University (Vice Chancellor Research Development Fund) and industry

sponsors BHP Billiton Ltd., Codelco, Geoinformatics Exploration Australia Pty. Ltd., Gold Fields Australasia Ltd., Jackaroo Drill Fund Pty. Ltd., Newmont Mining Corp., Placer Dome Asia Pacific Ltd., Teck Cominco Ltd., and WMC Resources Ltd. Last but not least we would like to thank the Reviewers Jon Hronsky and Gilpin Robinson for their insightful comments and valuable feedback, and the Guest Editor John Carranza for expert handling of this manuscript.

## References

- Agterberg, F.P., 2011. A modified weights-of-evidence method for regional mineral resource estimation. *Nat. Resour. Res.* 20, 95–101.
- Agterberg, F.P., Cheng, Q., 2002. Conditional independence test for weights-of-evidence modelling. *Nat. Resour. Res.* 11, 249–255.
- Apel, M., 2006. Predict – a Bayesian resource potential assessment plug-in for Gocad Available at: <http://www.geo.tu-freiberg.de/~apelm/predict.htm> (last accessed on: 06 April 2014).
- Billa, M., Cassard, D., Lips, A.L., Bouchot, V., Tourlière, B., Stein, G., Guillou-Frotter, L., 2004. Predicting gold-rich epithermal and porphyry systems in the central Andes with a continental-scale metallogenic GIS. *Ore Geol. Rev.* 25, 39–67.
- Bonham-Carter, G.F., 1994. *Geographic information systems for geoscientists: modelling with GIS*. Pergamon, Oxford (398 pp.).
- Bonham-Carter, G.F., Agterberg, F.P., 1990. Application of a microcomputer-based geographic information system to mineral-potential mapping. In: Hanley, J.T., Merriam, D.F. (Eds.), *Microcomputer-based Applications in Geology, II, Petroleum*. Pergamon Press, New York, pp. 49–74.
- Bonham-Carter, G.F., Agterberg, F.P., Wright, D.F., 1989. Weights of evidence modelling: a new approach to mapping mineral potential. In: Agterberg, F.P., Bonham-Carter, G.F. (Eds.), *Statistical Applications in the Earth Sciences*. Geological Survey of Canada 89-9, pp. 171–183.
- Bookstrom, A.A., Glen, R.A., Hammarstrom, J.M., Robinson Jr., G.R., Zientek, M.L., Drenth, B.J., Jaireth, S., Cossette, P.M., Wallis, J.C., 2014. Porphyry copper assessment of eastern Australia. U.S. Geological Survey Scientific Investigations Report, 2010-5090-L (160 pp.).
- Candela, P.A., Piccoli, P.M., 2005. Magmatic processes in the development of porphyry-type ore systems. In: Hedenquist, J.W., Thompson, J.F.H., Goldfarb, R.J., Richards, J.P. (Eds.), *Economic Geology 100th Anniversary Volume*, pp. 25–37.
- Carranza, E.J.M., 2009. Geochemical anomaly and mineral prospectivity mapping in GIS. *Handbook of Exploration and Environmental Geochemistry 11*. Elsevier, Amsterdam (351 pp.).
- Champion, D.D., Kositcin, N., Huston, D.L., Mathews, E., Brown, C., 2009. Geodynamic synthesis of the Phanerozoic of eastern Australia and implications for metallogeny. *Geoscience Australia Record*, 2009/18, (255 pp.).
- Clancy Exploration Limited, 2009. Company overview. Presentation to the Mining 2009 Resources Convention, Brisbane, October 28–30, 2009 (24 pp., Available at: [http://www.clancyexploration.com/Shared/Sites/clancyexploration/Assets/Your%20Files/company\\_presentations/Mining\\_2009\\_Resources\\_Convention\\_Presentation.pdf](http://www.clancyexploration.com/Shared/Sites/clancyexploration/Assets/Your%20Files/company_presentations/Mining_2009_Resources_Convention_Presentation.pdf) [last accessed on: 03 March 2014]).
- Cline, J.S., 2003. How to concentrate copper. *Science* 302, 2075–2076.
- Cooke, D.R., Wilson, A.J., House, M.J., Wolfe, R.C., Walshe, J.L., Lickfold, V., Crawford, A.J., 2007. Alkalic porphyry Au–Cu and associated mineral deposits of the Ordovician to Early Silurian Macquarie Arc, New South Wales. *Aust. J. Earth Sci.* 54, 445–463.
- Cowley, W.M., Katona, L.F., Gouthas, G., 2009. Assessment of mineral prospectivity of the northern Flinders Ranges using GIS analysis. *Primary Industries and Resources South Australia, Report Book 2009/19* (102 pp.).
- Cox, S.F., 1999. Deformational controls on the dynamics of fluid flow in mesothermal gold systems. In: McCaffrey, J.W., Lonergan, L., Wilkinson, J.J. (Eds.), *Fractures, Fluid Flow and Mineralization*. Geological Society of London, Special Publication 155, pp. 123–140.
- Cox, S.F., Knackstedt, M.A., Braun, J., 2001. Principles of structural control on permeability and fluid flow in hydrothermal systems. In: Richards, J.P., Tosdal, R.M. (Eds.), *Structural controls on ore genesis*. *Reviews in Economic Geology* 14, pp. 1–24.
- Crawford, A.J., Glen, R.A., Cooke, D.R., Percival, I.G., 2007. Geological evolution and metallogenesis of the Ordovician Macquarie Arc, Lachlan Orogen, New South Wales. *Aust. J. Earth Sci.* 54, 137–141.
- Deng, M., 2009. A conditional dependence adjusted weights of evidence model. *Nat. Resour. Res.* 18, 249–258.
- Fallon, M., Porwal, A.K., Guj, P., 2010. Prospectivity analysis of the Plutonic Marymia Greenstone Belt, Western Australia. *Ore Geol. Rev.* 38, 208–218.
- Feltrin, L., 2008. Predictive modelling of prospectivity for Pb–Zn deposits in the Lawn Hill Region, Queensland, Australia. *Ore Geol. Rev.* 34, 399–427.
- Feltrin, L., Baker, T., Scott, M., Fitzell, M., Wilkinson, K., 2008. A three-dimensional weights of evidence model for the Drummond basin in NE Queensland: Quantitative assessment of controlling variables for epithermal Au. *Australian Earth Sciences Convention (AESC) 2008*, Perth: New generation advances in geoscience, Abstracts, 89, p. 96.
- Fergusson, C.L., 2009. Tectonic evolution of the Ordovician Macquarie Arc, central New South Wales: arguments for subduction polarity and anticlockwise rotation. *Aust. J. Earth Sci.* 56, 179–193.
- Ford, A., Hart, C.J., 2013. Mineral potential mapping in frontier regions: a Mongolian case study. *Ore Geol. Rev.* 51, 15–26.
- Ford, A., Blenkinsop, T.G., 2008. Combining fractal analysis of mineral deposit clustering with weights of evidence to evaluate patterns of mineralization: application to copper deposits of the Mount Isa Inlier, NW Queensland, Australia. *Ore Geol. Rev.* 33, 435–450.

- Foster, D.A., Gray, D.R., 2000. Evolution and structure of the Lachlan Fold Belt (Orogen) of Eastern Australia. *Annu. Rev. Earth Planet. Sci.* 28, 47–80.
- Forster, D.B., Secombe, P.K., Phillips, D., 2004. Controls on skarn mineralization and alteration at the Cadia deposits, New South Wales, Australia. *Econ. Geol.* 99, 761–788.
- Forster, D.B., 2009. Pathways between skarns and porphyry deposits – a New South Wales perspective. Presentation to Exploration in the House 2009, NSW Parliament House Theatre, Canberra, June 18, 2009 (29 pp., Available at: [http://www.resources.nsw.gov.au/\\_data/assets/pdf\\_file/0007/289510/FORSTER\\_Skarn\\_and\\_porphyry\\_deposits\\_EITH2009.pdf](http://www.resources.nsw.gov.au/_data/assets/pdf_file/0007/289510/FORSTER_Skarn_and_porphyry_deposits_EITH2009.pdf) [last accessed on: 03 March 2014]).
- Geological Survey of New South Wales, 2006. Eastern Lachlan Orogen geoscience data (C146). DVD containing ESRI shapefiles and MapInfo tables Available at: <http://www.shop.nsw.gov.au/proddetails.jsp?publication=6866> (last accessed on: 08 April 2014).
- Glen, R.A., 2005. The Tasmanides of eastern Australia. In: Vaughan, A.P.M., Leat, P.T., Pankhurst, R.J. (Eds.), *Terrane Processes at the Margins of Gondwana*. Geological Society, London, Special Publications 246, pp. 23–96.
- Glen, R.A., Meffre, S., Scott, R.J., 2007a. Benambran orogeny in the eastern Lachlan orogen, Australia. *Aust. J. Earth Sci.* 54, 385–415.
- Glen, R.A., Crawford, A.J., Cooke, D.R., 2007b. Tectonic setting of porphyry Cu–Au mineralisation in the Ordovician–Early Silurian Macquarie Arc, Eastern Lachlan Orogen, New South Wales. *Aust. J. Earth Sci.* 54, 465–479.
- Glen, R.A., Saeed, A., Quinn, C.D., Griffin, W.L., 2011. U–Pb and Hf isotope data from zircons in the Macquarie Arc, Lachlan Orogen: Implications for arc evolution and Ordovician palaeogeography along part of the east Gondwana margin. *Gondwana Res.* 19, 670–685.
- Glen, R.A., Quinn, C.D., Cooke, D.R., 2012. The Macquarie Arc, Lachlan Orogen, New South Wales: its evolution, tectonic setting and mineral deposits. *Episodes* 35, 177–186.
- Golden Cross Resources Limited, 2013. Copper Hill focus on resource enhancement. Australian Securities Exchange (ASX) Release, 26 April 2013 pp., Available at: <http://www.goldencross.com.au/wp-content/uploads/260413.pdf> (last accessed on: 03 May 2014).
- González-Álvarez, I., Porwal, A., Beresford, S.W., McCuaig, T.C., Maier, W.D., 2010. Hydrothermal Ni prospectivity analysis of Tasmania, Australia. *Ore Geol. Rev.* 38, 168–183.
- Gray, N., Mandyczewsky, A., Hine, R., 1995. Geology of the zoned gold skarn system at Junction Reef, New South Wales. *Econ. Geol.* 90, 1533–1552.
- Harris, J.R., Wilkinson, L., Heather, K., Fumerton, S., Bernier, M.A., Ayer, J., Dahn, R., 2001. Application of GIS processing techniques for producing mineral prospectivity maps – a case study: mesothermal Au in the Swayze Greenstone Belt, Ontario, Canada. *Nat. Resour. Res.* 10, 91–124.
- Herbert, S., Woldai, T., Carranza, E.J.M., van Ruitenbeek, F., 2014. Predictive mapping of prospectivity for orogenic gold in Uganda. *J. Afr. Earth Sci.* <http://dx.doi.org/10.1016/j.jafrearsci.2014.03.001>.
- Holliday, J.R., Wilson, A.J., Blevin, P.L., Tedder, I.J., Dunham, P.D., Pfitzner, M., 2002. Porphyry gold–copper mineralisation in the Cadia District, Eastern Lachlan Fold Belt, New South Wales, and its relationship to shoshonitic magmatism. *Miner. Deposita* 37, 100–116.
- Hough, M.A., Bierlein, F.P., Wilde, A.R., 2007. A review of the metallogeny and tectonics of the Lachlan Orogen. *Miner. Deposita* 42, 435–448.
- Hronsky, J.M.A., 2004. The science of exploration targeting. SEG 2004 Conference, Perth, Centre for Global Metallogeny. University of Western Australia Publication 33, pp. 129–133.
- Hronsky, J.M.A., Groves, D.I., 2008. Science of targeting: definition, strategies, targeting and performance measurement. *Aust. J. Earth Sci.* 55, 3–12.
- Joly, A., Porwal, A.K., McCuaig, T.C., 2012. Exploration targeting for orogenic gold deposits in the Granites–Tanami Orogen: mineral system analysis, targeting model and prospectivity analysis. *Ore Geol. Rev.* 48, 349–383.
- Knox-Robinson, C.M., Wyborn, L.A.L., 1997. Towards a holistic exploration strategy: using geographic information systems as tool to enhance exploration. *Aust. J. Earth Sci.* 44, 453–463.
- Kreuzer, O.P., Etheridge, M.A., Guj, P., McMahon, M.E., Holden, D., 2008. Linking mineral deposit models to quantitative risk analysis and decision-making in exploration. *Econ. Geol.* 103, 829–850.
- Kreuzer, O.P., Etheridge, M.A., 2010. Risk and uncertainty in mineral exploration: implications for valuing mineral exploration properties. *Aust. Inst. Geosci. Newsl.* 100, 20–27.
- Kreuzer, O.P., Markwitz, V., Porwal, A.K., McCuaig, T.C., 2010. A continent-wide study of Australia's uranium potential – Part I: GIS-assisted manual prospectivity analysis. *Ore Geol. Rev.* 38, 334–366.
- Lawrie, K.C., Mernagh, T.P., Ryan, C.G., van Achtenbergh, E., Black, L.P., 2007. Chemical fingerprinting of hydrothermal zircons: an example from the Gidginbung high sulphidation Au–Ag–(Cu) deposit, New South Wales, Australia. *Proc. Geol. Assoc.* 118, 37–46.
- Lickfold, V., Cooke, D.R., Smith, S.G., Ullrich, T.D., 2003. Endeavour copper–gold porphyry deposits, Northparkes, New South Wales: Intrusive history and fluid evolution. *Econ. Geol.* 98, 1607–1636.
- Lickfold, V., Cooke, D.R., Crawford, A.J., Fanning, C.M., 2007. Shoshonitic magmatism and the formation of the Northparkes porphyry Cu–Au deposits, New South Wales. *Aust. J. Earth Sci.* 54, 417–444.
- Lindsay, M.D., Betts, P.G., Ailleres, L., 2014. Data fusion and porphyry copper prospectivity models, southeastern Arizona. *Ore Geol. Rev.* 61, 120–140.
- Lowell, J.D., Guilbert, J.M., 1970. Lateral and vertical alteration–mineralization zoning in porphyry ore deposits. *Econ. Geol.* 65, 373–408.
- Lord, D., Etheridge, M.A., Willson, M., Hall, G., Uttley, P.J., 2001. Measuring exploration success: an alternative to the discovery–cost–per-ounce method of quantifying exploration success. *Soc. Econ. Geol. Newsl.* 45 (1 and 10–16).
- Lusty, P.A.J., Scheib, C., Gunn, A.G., Walker, A.S.D., 2012. Reconnaissance-scale prospectivity analysis for gold mineralisation in the southern Uplands–Down–Longford Terrane, Northern Ireland. *Nat. Resour. Res.* 21, 359–382.
- Lye, A., Crook, G., van Oosterwijk, L.K., 2006. The discovery history of the Northparkes deposits. *Mineral Exploration Geoscience in New South Wales*. In: Lewis, P.C. (Ed.), *Mineral exploration geoscience in New South Wales*. Extended Abstracts, SMEDG Mines and Wines Conference, Cessnock, New South Wales, pp. 21–25.
- McCuaig, T.C., Hronsky, J.M.A., 2000. The current status and future of the interface between the exploration industry and economic geology research. In: Hagemann, S.G., Brown, P.E. (Eds.), *Gold in 2000*. Reviews in Economic Geology 13, pp. 553–559.
- McCuaig, T.C., Beresford, S., Hronsky, J.M.A., 2010. Translating the mineral systems approach into an effective exploration targeting system. *Ore Geol. Rev.* 38, 128–138.
- McGaughey, J., Perron, G., Parsons, S., Chalke, T., 2009. Gocad workflows for expert-system decision making. Proceedings of the 26th Gocad Research Conference, Nancy, France.
- Mejía-Herrera, P., Royer, J.J., Caumon, G., Cheillett, A., 2014. Curvature attribute from surface-restoration as predictor variable in Kupferschiefer copper potentials. An example from the Fore-Sudetic Region. *Nat. Resour. Res.* <http://dx.doi.org/10.1007/s11053-014-9247-7>.
- Newcrest Mining Limited, 2014. Annual mineral resources and ore reserves statement – 31 December 2013. Australian Securities Exchange (ASX) Release, 14 February 2014 38 pp., Available at: [http://www.newcrest.com.au/media/resource\\_reserves/2014/FINAL\\_December\\_2013\\_Resources\\_and\\_Reserves\\_Statement\\_140214.pdf](http://www.newcrest.com.au/media/resource_reserves/2014/FINAL_December_2013_Resources_and_Reserves_Statement_140214.pdf) (last accessed on: 03 May 2014).
- Nykänen, V., Groves, D.I., Ojala, V.J., Eilu, P., Gardoll, S.J., 2008. Reconnaissance-scale conceptual fuzzy-logic prospectivity modelling for iron oxide copper–gold deposits in the northern Fennoscandian Shield, Finland. *Aust. J. Earth Sci.* 55, 25–38.
- Partington, G.A., 2009. Commercial application of spatial data modelling with examples from North Queensland. AIG Northern Queensland Exploration and Mining Conference, Townsville, Australia, 3–8 (June) Available at: <http://www.kenex.co.nz/documents/papers/PartingtonNQEM2009.pdf> (last accessed on: 20 September 2014).
- Partington, G.A., Sale, M.J., 2004. Prospectivity mapping using GIS with publicly available earth science data – a new targeting tool being successfully used for exploration in New Zealand. Australasian Institute of Mining and Metallurgy Pacrim 2004 Congress Volume, Adelaide, 19–22 September 2004, p. 239–25.
- Partington, G.A., 2010. Developing models using GIS to assess geological and economic risk: an example from VMS copper–gold mineral exploration in Oman. *Ore Geol. Rev.* 38, 197–207.
- Porwal, A.K., Kreuzer, O.P., 2010. Introduction to the special issue: mineral prospectivity analysis and quantitative resource estimation. *Ore Geol. Rev.* 38, 121–127.
- Porwal, A.K., González-Álvarez, I., Markwitz, V., McCuaig, T.C., Mamuse, A., 2010. Weights of evidence and logistic regression modeling of magmatic nickel sulfide prospectivity in the Yilgarn Craton, Western Australia. *Ore Geol. Rev.* 38, 184–196.
- Raines, G.L., Bonham-Carter, G.F., Kemp, L., 2000. Predictive probabilistic modelling using ArcView GIS. *ArcUser Mag.* 2, 45–48 (Available at: <http://www.esri.com/news/arcuser/0400/files/wofe.pdf> [last accessed on: 08 March 2014]).
- Richards, J.P., 2003. Tectono-magmatic precursors for porphyry Cu–(Mo–Au) deposit formation. *Econ. Geol.* 98, 1515–1533.
- Roscoe, W.E., 2002. Valuation of mineral exploration properties using the cost approach. Special session on valuation of mineral properties, PDAC/CIM Millennium 2000 Conference, March 8, Toronto, Canada (Available at: [http://thamdinghia.org/uploads/1/valdaybill\\_roscoe.pdf](http://thamdinghia.org/uploads/1/valdaybill_roscoe.pdf) [last accessed on: 03 May 2014]).
- Rose, P.R., 1999. Taking the risk out of petroleum exploration: the adaptation of systematic risk analysis by international corporations during the 1990s. *Lead. Edge* 18, 192–199.
- Schmitt, E., 2010. Weights of evidence mineral prospectivity modelling with ArcGIS. EOSC 448 – Directed Studies. Department of Earth, Ocean & Atmospheric Studies, University of British Columbia, Vancouver (65 pp., Available at: [http://www.mdr.ubc.ca/home/courses/SC62\\_GIS/ESchmitt\\_EOSC448\\_DirStudies.pdf](http://www.mdr.ubc.ca/home/courses/SC62_GIS/ESchmitt_EOSC448_DirStudies.pdf) [last accessed on: 04 April 2014]).
- Seedorff, E., Dilles, J.H., Proffett, J.M., Einaudi, M.T., Zurcher, L., Stavast, W.J.A., Johnson, D.A., Barton, M.D., 2005. Porphyry deposits: characteristics and origin of hypogene features. In: Hedenquist, J.W., Thompson, J.F.H., Goldfarb, R.J., Richards, J.P. (Eds.), *Economic Geology 100th Anniversary Volume*, pp. 251–298.
- Sawatzky, D.L., Raines, G.L., Bonham-Carter, G.F., 2010. Spatial data modeller Available at: <http://www.ige.unicamp.br/sdm/ArcSDM10/source/ReadMe.pdf>.
- Sillitoe, R.H., 2000. Gold-rich porphyry deposits, descriptive and genetic models and their role in exploration and discovery. In: Hagemann, S.G., Brown, P.E. (Eds.), *Gold in 2000*. Reviews in Economic Geology 13, pp. 315–345.
- Sillitoe, R.H., 2010. Porphyry copper systems. *Econ. Geol.* 105, 3–41.
- Smith, P., 2012. Cadia Valley. The Australasian Institute of Mining and Metallurgy Sydney Branch Presentation, 01 November 2012, Sydney, New South Wales (Available at: [http://www.ausim.com.au/content/docs/branch/sydney\\_2012\\_11\\_01\\_presentation.pdf](http://www.ausim.com.au/content/docs/branch/sydney_2012_11_01_presentation.pdf) [last accessed on: 08 March 2014]).
- Spiegelhalter, D.J., 1986. Uncertainty in expert systems. In: Gale, W.A. (Ed.), *Artificial Intelligence and Statistics*. Addison-Wesley, Massachusetts, p. 17–15.
- Suppel, D.W., Scheibner, W., 1990. Lachlan Fold Belt in New South Wales – regional geology and mineral deposits. In: Hughes, F.E. (Ed.), *Geology of the Mineral Deposits of Australia and Papua New Guinea*. The Australian Institute of Mining and Metallurgy Monograph 14, pp. 1321–1327.
- Suslick, S.B., Schiozer, D.J., 2004. Risk analysis applied to petroleum exploration and production: an overview. *J. Pet. Sci. Eng.* 44, 1–9.
- Thomas, M., Moorehead, C., 2011. Technical report on the Cadia Valley Operations project in New South Wales, Australia. NI 43-101 Report prepared for Newcrest Mining

- Limited. AMC Mining Consultants (Canada) Limited (135 pp., Available at: [http://www.newcrest.com.au/media/resource\\_reserves/Technical%20Reports/FINAL\\_\(a4\)\\_Technical\\_Report\\_Cadia\\_Valley\\_Property\\_December\\_31\\_2011.pdf](http://www.newcrest.com.au/media/resource_reserves/Technical%20Reports/FINAL_(a4)_Technical_Report_Cadia_Valley_Property_December_31_2011.pdf) [last accessed on: 08 March 2014]).
- Tosdal, R.M., Richards, J.P., 2001. Magmatic and structural controls on the development of porphyry Cu ± Mo ± Au deposits. In: Richards, J.P., Tosdal, R.M. (Eds.), *Structural Controls on Ore Genesis*. *Reviews in Economic Geology* 14, pp. 157–181.
- Tripp, G.I., Vearncombe, J.R., 2004. Fault/fracture density and mineralization: a contouring method for targeting in gold exploration. *J. Struct. Geol.* 26, 1087–1108.
- Walshe, J.L., Heithersay, P.S., Morrison, G.W., 1995. Toward an understanding of the metallogeny of the Tasman Fold Belt System. *Econ. Geol.* 90, 1382–1401.
- Wang, G., Carranza, E.J.M., Zuo, R., Hao, Y., Du, Y., Pang, Z., Sun, Y., Qu, J., 2012. Mapping of district-scale potential targets using fractal models. *J. Geochem. Explor.* 122, 47–54.
- Wastell, C.A., Etheridge, M.A., McMahon, M.E., Lucas, G., Hartley, L., 2011. The impact of cognitive predispositions on exploration decisions in the minerals industry. *Appl. Cogn. Psychol.* 25, 469–479.
- Wilkinson, J.J., 2013. Triggers for the formation of porphyry ore deposits in magmatic arcs. *Nat. Geosci.* 6, 917–925.
- Wilson, A.J., Cooke, D.R., Stein, H.J., Fanning, C.M., Holliday, J.R., Tedder, I.J., 2007. U–Pb and Re–Os geochronologic evidence for two alkalic porphyry ore-forming events in the Cadia District, New South Wales, Australia. *Econ. Geol.* 102, 3–26.
- Winter, J.D., 2001. *An introduction to igneous and metamorphic petrology*. Prentice Hall, (697 pp.).
- Wyborn, L.A.I., Heinrich, C.A., Jaques, A.L., 1994. Australian Proterozoic mineral systems: essential ingredients and mappable criteria. *Australas. Inst. Min. Metall. Publ. Ser.* 5, 109–115.